Nanoscale

FEATURE ARTICLE

View Article Online
View Journal | View Issue

Cite this: *Nanoscale*, 2015, **7**, 7502

Engineering noble metal nanomaterials for environmental applications

Jingguo Li,†[a] Tingting Zhao,†[a] Tiankai Chen,[a] Yanbiao Liu,*[b] Choon Nam Ong[b] and Jianping Xie*[a]

Besides being valuable assets in our daily lives, noble metals (namely, gold, silver, and platinum) also feature many intriguing physical and chemical properties when their sizes are reduced to the nano- or even subnano-scale; such assets may significantly increase the values of the noble metals as functional materials for tackling important societal issues related to human health and the environment. Among which, designing/engineering of noble metal nanomaterials (NMNs) to address challenging issues in the environment has attracted recent interest in the community. In general, the use of NMNs for environmental applications is highly dependent on the physical and chemical properties of NMNs. Such properties can be readily controlled by tailoring the attributes of NMNs, including their size, shape, composition, and surface. In this feature article, we discuss recent progress in the rational design and engineering of NMNs with particular focus on their applications in the field of environmental sensing and catalysis. The development of functional NMNs for environmental applications is highly interdisciplinary, which requires concerted efforts from the communities of materials science, chemistry, engineering, and environmental science.

Received 6th February 2015,
Accepted 25th March 2015

DOI: 10.1039/c5nr00857c

www.rsc.org/nanoscale

1. Introduction

The rapid population growth and fast urbanization and industrialization have caused serious environmental issues that we are currently facing. These issues may become even worse if no efficient/sustainable solutions can be found.[1] In particular, environmental monitoring and control have already become a major issue of global concern. Although some advanced analytical techniques, such as chromatography-mass spectrometry (LC/MS/MS and GC/MS), are capable of detecting

[a]*Department of Chemical and Biomolecular Engineering, National University of Singapore, 117585 Singapore, Singapore. E-mail: chexiej@nus.edu.sg; Fax: +65 6516 1936; Tel: +65 6516 1067*
[b]*NUS Environmental Research Institute, National University of Singapore, 5A Engineering Drive 1, #02-01, 117411 Singapore, Singapore. E-mail: eriliuyb@nus.edu.sg; Fax: +65 6872 1320; Tel: +65 6601 3302*
† These two authors contributed equally to this work.

Jingguo Li

Jingguo Li received his B.S. from Henan University and M.S. from the University of Science and Technology of China, China. He is currently a PhD student at the Department of Chemical and Biomolecular Engineering, National University of Singapore (NUS), under the supervision of Prof. Jianping Xie. His research interest is design of nanocomposite membrane for water treatment.

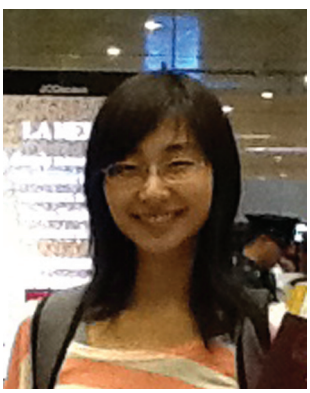

Dr Tingting Zhao

Dr Tingting Zhao received her PhD degree in Chemistry from the National University of Singapore (NUS). She is currently a postdoctoral fellow in Prof. Jianping Xie's group at the Department of Chemical and Biomolecular Engineering, NUS. Her research interests are design of silica-coated metal nanoclusters for catalytic and biomedical applications.

various trace pollutants, the high equipment and maintenance costs and the requirement of professional operators have constrained their practical applications. Therefore, there is a pressing need to develop highly sensitive, selective, rapid, cost-effective, and miniature sensor systems for the detection of environmental pollutants.[2] Besides the accurate quantification of pollutants, the removal of various environmental pollutants is also of paramount interest to the environmental community; however, it is technically challenging. Conventional treatment technologies (*e.g.*, adsorption) may not be effective for the removal, conversion and/or degradation of some refractory pollutants,[3] and most of the traditional treatment technologies such as membrane technology are often energy-intensive.[4] Therefore, the development of efficient and cost-effective pollutant control technologies is highly desirable.

Recent advances in noble metal nanomaterials (NMNs) may provide promising solutions for the above mentioned environmental issues.[5–7] In particular, the intriguing physical and chemical (or physicochemical) properties of NMNs can be readily used to develop good platforms for a variety of environmental applications, such as sensor development for environmental pollutants and catalytic decomposition of pollutants. In addition, the design of functional NMNs will go back to the hand of materials chemists, since with delicate design of the chemistry involved, the physicochemical properties of NMNs can be controlled in a good manner by tailoring the attributes of NMNs, such as size, shape, composition, and surface.[8–10] For example, it has been proven that the optical properties (*e.g.*, surface plasmon resonance (SPR) or fluorescence) of NMNs can be adjusted by their particle size.[11]

The intriguing properties of NMNs have already been used for many environmental applications. One such application is to use the catalytic properties of NMNs for the removal and decomposition of pollutants. A number of studies have suggested that some NMNs possess better selectivity and activity than transition metals in many environmental-related catalytic reactions, such as the oxidation of carbon monoxide (CO)[12,13] and volatile organic compounds (VOCs).[14,15] The rapid development of this field is also reflected by the increase of publications over the years and the publication of a number of comprehensive reviews on this topic.[16–21] Most of the recent reviews focused their discussions on the controlled synthesis of NMNs and their biomedical[22,23] and energy applications.[5,21,24,25] It is therefore timely to present a feature article on the recent development of NMNs with a particular focus on their environmental applications, which will be of interest to a broad readership in environmental science, engineering, analytical chemistry, and materials science. In this article, we focus our discussion on the recent progress in the rational designing and engineering of NMNs for environmental sensing and catalysis applications. In the next section, we will first discuss the unique properties that we could achieve from NMNs by engineering their attributes such as size, shape, composition, and surface, followed by a brief discussion on how to correlate the physicochemical properties of NMNs to their performance in environmental applications.

2. Why noble metal nanomaterials?

NMNs such as gold (Au), silver (Ag), and platinum (Pt) often feature unique and tunable electrical, optical, and chemical properties; such properties have attracted great interest of the community to design functional NMNs for both basic and applied research in the environmental field. Operating in the nanoscale size region, the properties of NMNs are distinctively different from their atomic constituents and bulk substances due to their high surface-to-volume ratio and quantum size effects.[21] In particular, the physicochemical properties of NMNs are dictated by their attributes like size, shape, architecture, crystallinity, and composition. These key attributes can be used to tailor the functionalities of NMNs and their performance in practical applications.[24,26,27] Recent advances in the synthetic chemistry of NMNs have provided good protocols to produce NMNs with well-controlled attributes in quantities large enough for practical applications. For example, NMNs with different shapes, such as rods,[28] wires,[29] spheres,[30] cubes,[26] plates,[31] belts,[32,33] and cages,[34] have been successfully

Tiankai Chen

Tiankai Chen received his B.S. degree in materials chemistry from Peking University, China, in 2014. After that, he joined Prof. Jianping Xie's group as a PhD student at the Department of Chemical and Biomolecular Engineering, National University of Singapore (NUS). He is interested in developing novel nanomaterials for environmental applications.

Dr Yanbiao Liu

Dr Yanbiao Liu received his PhD degree in environmental science from Shanghai Jiao Tong University of China (in 2012). He is currently a Research Scientist at the NUS Environmental Research Institute (NERI). His current research interests are environmental functional materials with a focus on the development of electrochemical graphene filters for water purification and photocatalysis.

produced by some wet chemical protocols. In addition, the biological and biomimetic synthesis of NMNs using biomaterials as living "nanofactories" have received recent attention to address the fundamental principles of green chemistry.[35] These biomaterials include organisms (*e.g.*, bacteria and fungi and biomass) and mixed biomolecules from the organisms, proteins, and peptides.[16] For example, Das *et al.* developed a controlled synthesis protocol of multi-shaped Au NPs at room temperature by the interaction of Au salts (*e.g.*, $HAuCl_4{\cdot}3H_2O$) with the cell-free extract of a fungal strain *Rhizopus oryzae*. Various shapes of Au NPs, such as triangular, hexagonal, pentagonal, spherical, spheroidal, urchin-like, nanowires, and nanorods, can be obtained by tailoring the reaction parameters, such as the precursor concentration, solution pH, and reaction time.[36] The as-synthesized bio-integrated NPs possessed very high adsorption capacity towards various contaminants (*e.g.*, organophosphorus pesticides and dyes) and exhibited high antibacterial activity against several Gram-negative (*e.g.*, *Escherichia coli*) and Gram-positive (*e.g.*, *Bacillus subtilis*) bacteria and yeasts (*e.g.*, *Saccharomyces cerevisiae*).[37–39] It has been well-demonstrated that the size and shape of NMNs are two determinant factors for their catalytic activity.[25] There are several interesting review articles on this topic, and readers may refer to these papers for more information about this field of research.[5,6,21,23]

By continually decreasing the size of NMNs to below 2 nm, we observe distinctive changes in the physical and chemical properties of the particles. These sub-2 nm sized particles form a unique class of nanomaterials, often described as metal nanoclusters (NCs). In recent years, the research on sub-2 nm metal NCs has been intensively pursued due to its unique role in bridging the "missing link" between single metal atoms and relatively large metal nanoparticles (NPs with particle sizes above 2 nm).[40–47] Metal NCs typically contain several to a hundred metal atoms, and they are stabilized by a particular organic ligand such as thiolates and proteins. Among the newly developed metal NCs, thiolate-protected NCs or thiolated NCs are the most common class of NCs. This type of NCs can be denoted as $M_n(SR)_m$, where M is the noble metal, SR is the thiolate ligand, and n and m are specific integers. Recently, a number of efficient synthetic strategies have been developed to produce atomically precise thiolated Au/Ag NCs.[48–63] These newly developed synthetic strategies can be used to tailor the physicochemical (*e.g.*, optical and catalytic) properties of metal NCs. In addition, due to its ultra-small size feature, the contribution of even one additional atom or ligand is greatly amplified in metal NCs, leading to the high size sensitivity of the physicochemical properties of NCs. More interestingly, metal NCs feature discrete and size-dependent electronic states, showing some unique molecular-like properties, such as HOMO–LUMO transition, quantized charging, and strong fluorescence; such properties are distinctively different from their larger counterparts—NPs with core sizes more than 2 nm—and these properties can be readily used for many applications in the environmental field.[55,64]

One can visualize the synthesis of NMNs as an engineerable process, where the input is the precursors for NMNs synthesis and the output is the NMNs with pre-designed properties (*e.g.*, optical and catalytic) that are particularly required in an environmental application. The conversion from input to output can be delicately controlled by its conversion chemistry. As illustrated in Scheme 1, there are three major strategies to tailor the physicochemical properties of NMNs. The first strategy is to tailor the size and shape of NMNs; many successful demonstrations exist for this. For example, Link and El-Sayed have shown the size dependence of the SPR absorption of Au NPs.[65] Similarly, the properties of metal NCs are also size-dependent. For example, the fluorescence properties of Ag NCs can be tuned by adjusting the cluster size.[66] Shape is another crucial factor that could affect the optical properties of NMNs. For example, unlike the visible SPR absorption of spherical Au NPs, the SPR peaks of the Au nanocages could be tuned in the range of visible and near-infrared (NIR).[26]

The second strategy is to tailor the composition of NMNs. Among which, the synthesis of alloyed NMNs is an efficient

Prof. Choon Nam Ong

Prof. Choon Nam Ong received his PhD degree from the University of Manchester in 1997 and he is currently a Professor in the Saw Swee Hock School of Public Health at the National University of Singapore (NUS) and he is also the Director of NUS Environmental Research Institute (NERI). He has published over 300 scientific papers with an H*-index of 70 and ~15 000 citations and his main research interest is environmental health and toxicology.*

Dr Jianping Xie

Dr Jianping Xie received his B.S. and M.S. in Chemical Engineering from Tsinghua University, China. He graduated with PhD from the Singapore-MIT Alliance (SMA) program. He joined National University of Singapore (NUS) as an Assistant Professor in 2010. His current research interests are engineering ultra-small noble metal nanoclusters for biomedical and environmental applications.

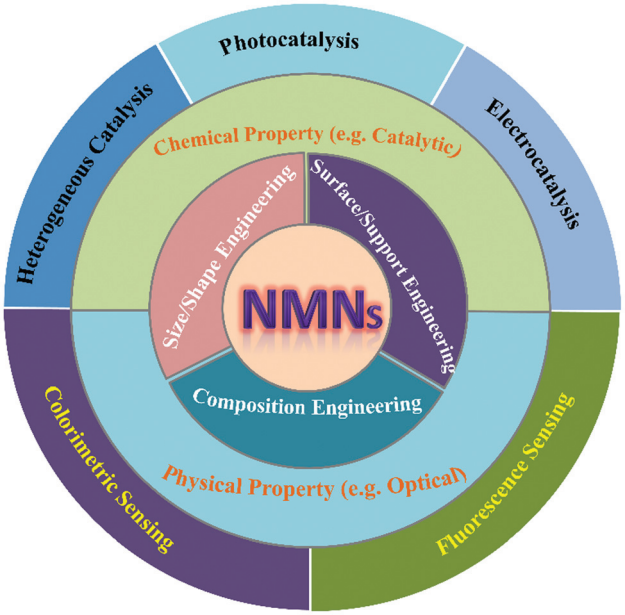

Scheme 1 Schematic illustration of three strategies that can be used to tailor the physicochemical properties of NMNs, and the use of these physicochemical properties for several emerging applications in the environmental field.

way to further enrich the optical or catalytic properties of NMNs. In addition, by doping an inexpensive metal element such as Ag and Cu to the NMNs, the cost of the as-designed NMNs will be more competitive for many practical applications. For example, we have recently developed an efficient strategy to dope different amounts of Ag atoms to thiolated Au_{25} NCs, leading to the formation of Au_xAg_{25-x} NCs featuring different optical absorptions.[67]

The third strategy is to tailor the surface and support of NMNs, where the functional groups or ligands on the NMN surface as well as the supporting materials for NMNs can be readily used to adjust the physicochemical properties of NMNs. For example, protecting ligands have a pronounced effect on the physicochemical properties of metal NCs.[68] In addition, the choice of the ligands and supports may also affect other physicochemical properties of the as-designed NMNs (*e.g.*, electric conductivity).[58]

Development of highly sensitive and selective sensors for environmental pollutant detection requires both the development of technology and fundamental knowledge in chemistry, biology, and materials science. To construct a good sensor, two key components are required: a recognition element to provide selective and specific interaction with the target analytes and a transducer component for signalling the blinding event.[69] A good sensor often relies on the abovementioned two elements of the recognition process in terms of response time, signal-to-noise (S/N) ratio, selectivity, and sensitivity. Therefore, the design of good sensors is highly dependent on the quality and properties of functional materials used in the construction of the sensors. NMNs possess unique physicochemical properties (*e.g.*, size-dependent SPR or fluorescence), which could be used to develop sensors for various analytes such as heavy metal ions. In particular, Au and Ag nanomaterials have attracted extensive research interest because they exhibit exceptionally high absorption and scattering coefficients in the UV-vis-NIR range, making them the most attractive candidates for colorimetric and fluorometric sensor development.[9,70] More details will be discussed in section 3, suggesting the rational design of NMNs for the development of optical sensors for environmental pollutants.

In addition, NMNs have recently emerged as promising catalysts for the conversion and/or decomposition of some environmental pollutants. In particular, the electron deficiency of Pt and Au NPs may facilitate their strong affinity with some molecules such as oxygen, making them promising for various catalytic applications. The incorporation of NMNs into next-generation catalysts for environmental applications can be broadly classified into three categories: heterogeneous catalysis, photocatalysis, and electrocatalysis. It has been well-documented that the attributes of NMNs determine their catalytic performance. The design and use of NMN-based catalysts for environmental applications will be discussed in section 4.

3. Sensing applications of NMNs

Recent environmental burdens caused by industrial and agricultural wastes have attracted growing concern in the community.[71] Among these hazardous pollutants (*e.g.*, heavy metal ions, pesticides, dyes, toxic chemicals, pathogens, nanomaterials, and contaminants),[72,73] heavy metal ions have attracted the most attention due to their serious threat to human health and the environment.[74] For an accurate quantification of these heavy metal ions, various optical sensors constructed from NMNs,[22,69,75,76] organic dyes,[77,78] and fluorescent polymers,[79] have been demonstrated. Among the functional materials used for the sensor design, NMNs are the most attractive due to their intriguing physical and chemical properties, including size and shape dependent optical properties, high surface area, good stability, and good biocompatibility.[75,80,81] In particular, NMNs with core sizes greater than 5 nm exhibit strong SPR absorption.[11] The SPR properties of NMNs may change in the presence of analytes, which could induce the aggregation of NMNs in the solution; this distance-dependent SPR property can be readily used to design a colorimetric sensor. On the other hand, metal NCs with core sizes below 2 nm feature strong fluorescence, and the fluorescence properties of NCs may also be sensitive to some analytes; the fluorescence change (turn-on or turn-off) can then be used to design a fluorometric sensor.[75,76] Herein, we will use heavy metal ions as a model analyte to discuss recent advances in the design of NMNs for the development of optical sensors.

3.1 Colorimetric sensor

NMNs-based colorimetric sensor has attracted increasing attention due to the high extinction coefficient of NMNs,

which is typically several orders of magnitude higher than that of organic dyes.[82] The colorimetric response can be easily monitored by the naked eye or UV-vis spectrometer, and the colorimetric method provides a simple, cost effective, and promising procedure for the sensitive and selective detection of various environmental pollutants such as heavy metal ions. It is well-documented that the SPR properties of NMNs are strongly influenced by their size, shape, composition, and surface (or ligands on particle surface). Thus, one could tune these attributes to achieve the desirable SPR properties of NMNs that can be used to construct a colorimetric sensor for the detection of environmental pollutants.

3.1.1 Size and shape matters. In general, NMNs display intense colors in solution owing to the collective oscillation of conductive electrons upon their interactions with the visible light. The SPR peaks of NMNs are highly dependent on their size and shape, which typically shift to a longer wavelength when the particle size increases, as indicated in Fig. 1.[65,83,84] For example, Chai *et al.* synthesized Au NPs with core sizes of 5–8 nm,[85] which showed a characteristic SPR peak at ~520 nm with an extinction coefficient of 5×10^7 cm^{-1} mol^{-1} L.[86] The as-prepared Au NPs were protected by glutathione (GSH). The GSH-Au NPs could immediately aggregate in the presence of Pb^{2+} in solution, showing good sensitivity to Pb^{2+} (a limit of detection or LOD of 100 nM) and superior selectivity of Pb^{2+} over other metal ions including Hg^{2+}, Mg^{2+}, Zn^{2+}, Ni^{2+}, Cu^{2+}, Co^{2+}, and Ca^{2+}. As the size of Au NPs increased to 13 nm, the extinction coefficient of Au NPs further increased to 2×10^8 cm^{-1} mol^{-1} L. As a result, the sensitivity of this sensor system was further improved. In a separate study, a (11-mercapto-undecyl)-trimethylammonium (MTA)-protected Au NP of ~13 nm was used to construct a sensor to detect Hg^{2+} in acidic conditions.[87] The solution color of the Au NPs changed from red to blue in the presence of Hg^{2+}, which was also reflected in their UV-vis absorption spectra, showing an obvious red shift of the absorption peak. The red shift of the SPR peaks was induced by the aggregation of Au NPs in solution due to the high affinity of MTA towards Hg^{2+}, which could trigger the breakage of Au–S bonds on the NP surface. A high sensitivity and selectivity for Hg^{2+} was therefore achieved in this sensor system. The high affinity between Au NPs and Hg^{2+} can also be utilized to remove mercury from water. For example, Lisha *et al.* designed a novel, low-cost, recyclable and high-performance Au NPs-Al_2O_3 composite adsorbent for the removal of Hg from drinking water.[88] A high loading capacity of 4.065 g g^{-1} Au NPs was obtained, and this good performance was attributed to the Au–Hg amalgam and the formation of amorphous Hg layer over the Au NP surface. In addition, the data suggests that only 738 mg of Au NPs was required to treat 3500 L of 1 ppm Hg, which could be promising for practical applications.

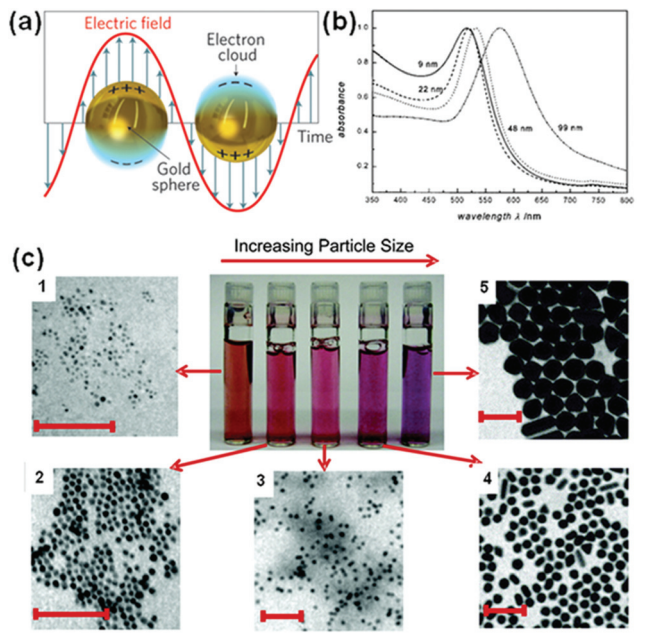

Fig. 1 (a) Schematic illustration of the collective oscillation of electrons with the incident electromagnetic field in Au NPs. Reprinted with permission from ref. 83. Copyright (2011) Nature Publishing Group. (b) Optical absorption spectra of spherical Au NPs with particle sizes of 9, 22, 48, and 99 nm. Reprinted with permission from ref. 65. Copyright (1999) American Chemical Society. (c) Digital images and corresponding TEM images of spherical Au NPs with different sizes of 4–40 nm (scale bar of 100 nm). Reprinted with permission from ref. 84. Copyright (2006) American Chemical Society.

The shape of metal NPs may also affect the sensor performance. For example, a decahedral Au NP was recently synthesized by a simple solar-mediated method,[89] which showed good sensor performance for detecting Pb^{2+} ions in solution. The LOD demonstrated in this study was 5 nM, which is 1000-fold lower than that of 13 nm Au NP system.[85] More recently, Ag NPs with different shapes, such as nanospheres, nanoplates, and nanorods, were used to construct colorimetric sensors for Co^{2+}. It was found that the spherical Ag NPs showed the highest sensitivity for Ni^{2+}, Co^{2+}, Cd^{2+}, Pb^{2+}, and As^{3+}.[90] However, the Ag nanorods showed a specific response to Co^{2+} over other interfering metal ions in the solution, which could be attributed to the cooperative effect of two protecting ligands on the NP surface (surfactant (CTAB) and glutathione (GSH)). The abovementioned examples suggest the crucial roles of size and shape of NMNs in the design of colorimetric sensors for heavy metal ions.

3.1.2 Composition matters. Once the composition of the core changes, the extinction coefficients of NMNs may also change, which could affect the sensitivity of the sensors for heavy metal ions. For example, 13 nm Au NPs possess a high extinction coefficient (2×10^8 cm^{-1} mol^{-1} L),[87] which is considerably higher than that of traditional chromophores. Therefore, the analyte-induced aggregation of Au NPs could be used to design sensors for various environmental pollutants. For example, a label-free Au NP sensor was developed for the detection of Hg^{2+} ions in aqueous solutions.[91] High specificity and sensitivity was observed due to the specific and strong interaction of 4-mercaptobutanol with Au and Hg^{2+} as well as

the metallophilic interaction of Hg^{2+} and Au^{+}. In particular, the aggregation extent of Au NPs decreased upon the introduction of Hg^{2+}. It should be noted that Ag NPs have a higher molar extinction coefficient than Au NPs; it is about 100-fold higher.[92] This property could be used to further improve the sensitivity of the optical sensors. For example, a simple and cost-effective assay was developed using mercury-specific oligonucleotides and label-free Ag NPs to construct a colorimetric sensor for Hg^{2+}.[93] In the presence of Hg^{2+}, the unfolded thymine (T)-rich oligonucleotides were linked with Hg^{2+} to form a stem–loop structure. As a result, the hairpin structure of oligonucleotides could not protect and stabilize the Ag NPs, leading to the aggregation of Ag NPs in solution. More recently, a citrate-protected Pt NP was used to construct a colorimetric sensor for Hg^{2+}.[94] The as-prepared Pt NPs could catalyze the reaction between 3,3′,5,5′-tetramethylbenzidine and H_2O_2, leading to the formation of a blue color product. However, the catalytic activity of Pt NPs could be largely inhibited by a trace amount of Hg^{2+}, as shown in Fig. 2. The above-mentioned examples suggest that the composition control of NMNs is an efficient way to design a good colorimetric sensor for environmental pollutants.

3.1.3 Ligand shell matters. The SPR properties of NMNs are highly sensitive to their ligand shell. Recently, NMNs functionalized with different organic ligands (*e.g.*, thiolates, amino acids, peptides, and DNA) have been demonstrated as effective colorimetric sensors for various heavy metal ions.[85,91] For example, Sener *et al.* reported a colorimetric assay based on the aggregation of citrate-protected Au NPs in the presence of Hg^{2+} and lysine.[95] Hg^{2+} ions were first adsorbed on the Au NP surface, forming a strong Hg^{2+}–Au bond. As a result, the color of the NP solution changed from red to purple or gray upon the addition of lysine (Fig. 3). In a separate study, peptide-functionalized Au NPs were synthesized and used to construct a sensor for Co^{2+}, Hg^{2+}, Pb^{2+}, Pd^{2+}, and Pt^{2+}.[96] The colorimetric response was rapid (<1 min) and the sensor was sensitive.

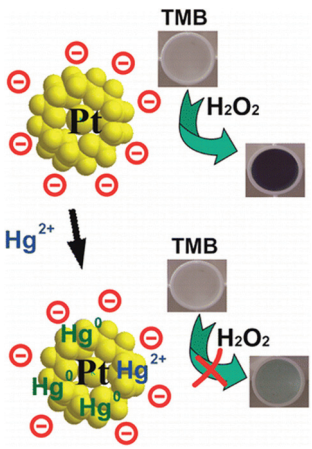

Fig. 2 Proposed mechanism for Hg^{2+}-induced colorimetric response of Pt NPs. Reprinted with permission from ref. 94. Copyright (2014) American Chemical Society.

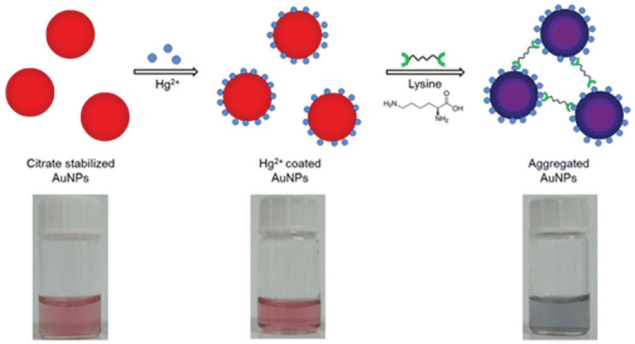

Fig. 3 Proposed Hg^{2+} sensing mechanism of the colorimetric assay (top panel) and the digital images of Au NP solutions (bottom panel), showing that the color only changed in the presence of lysine (0.4 mM) and Hg^{2+} (10 μM). Reprinted with permission from ref. 95. Copyright (2014) American Chemical Society.

Recently, DNA-modified Au NPs have been used to construct colorimetric sensors for heavy metal ions such as Hg^{2+}. For example, the thymine (T) base in DNA sequence can interact with Hg^{2+} to form a T–Hg^{2+}–T coordination, which could be used for designing a sensor for Hg^{2+}.[97] In addition, the DNA sequence can be further modified and optimized (*e.g.*, with an optimized number of T units) to detect Hg^{2+} even at room temperature.[98] The examples discussed in this section justify the importance of the ligand shell on the NP surface for designing optical sensors for heavy metal ion detection.

3.2 Fluorometric sensor

The unique fluorescence properties of noble metal NCs make them attractive for the detection of heavy metal ions owing to their good water solubility, large Stokes shifts, low toxicity, and high emission rates.[99,100] Because the fluorescence properties of NCs are largely dictated by the attributes of the NC, one can tailor the size, composition, structure, and surface of NCs to adjust their fluorescence properties, and thus optimize the sensor systems to realize a desirable performance. There are several recent reviews on the use of Au/Ag NCs for sensor applications.[19,22,69,76,99,101] Herein, we will summarize recent advances in the design of fluorescent metal NCs for sensor development, particularly for the detection of environmental pollutants such as heavy metal ions.

3.2.1 Core size matters. The fluorescence properties of metal NCs are size dependent, as suggested in the system of NCs protected by poly(amidoamine) (PAMAM) (Fig. 4).[102] Besides the size of NCs, the fraction of active metal species (Au^{+} or Ag^{+}) on the NC surface is also crucial for the fluorescence properties of metal NCs. In general, metal NCs with smaller sizes (or fewer metal atoms) often feature higher fluorescence owing to their smaller size and larger surface area (or large fraction of active metal species (Au^{+} or Ag^{+})).[19] The fluorescent metal NCs have recently emerged as a new class of promising fluorescent probes for the development of optical sensors for environmental pollutant detection. For example,

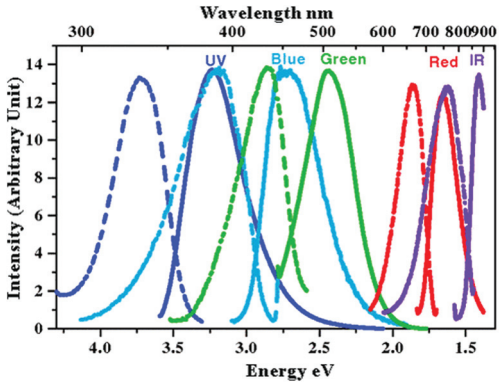

Fig. 4 Photoexcitation (dashed lines) and photoemission (solid lines) spectra of fluorescent Au NCs protected by dendrimers, showing a size-dependent emission property. Reprinted with permission from ref. 102. Copyright (2004) American Physical Society.

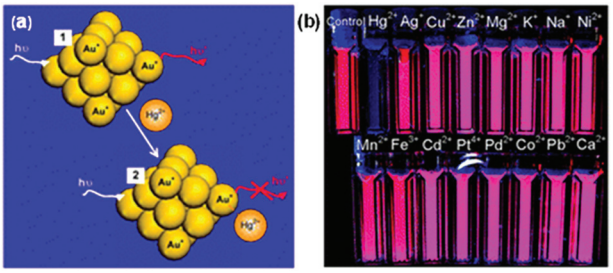

Fig. 5 (a) Schematic illustration of the metallophilic Hg^{2+}–Au^{+} interaction induced quenching of the fluorescence of Au NCs. (b) Digital images of aqueous Au NC solutions (20 μM) under UV light in the presence of 50 μM of various metal ions, showing an excellent selectivity of the Au NC-based sensor for Hg^{2+} over other interfering metal ions. Reprinted with permission from ref. 109. Copyright (2010) Royal Society of Chemistry.

a well-developed $Au_{25}(SG)_{18}$ species was recently used to construct a fluorometric sensor for Ag^{+}, which showed good sensitivity and selectivity.[103] In another study, a highly fluorescent Au NC protected by lysozyme (with ~43% Au^{+} on the NC surface) was used for the detection of Hg^{2+} and CH_3Hg^{+} with the LOD of 3 pM and 4 nM, respectively.[104] Similarly, a bovine serum albumin (BSA)-protected Au_{16} NC species was successfully synthesized *via* a microwave-reduction protocol, and this NC species was used to construct a fluorescence-enhancement sensor for the detection of trace Ag^{+} ions.[105] It was observed that the deposition of Ag^{+} (or Ag^{0}) on the Au_{16} NC surface could lead to the formation of Ag–Au alloy NCs, which could greatly increase the fluorescence intensity of the Au NCs in solution. Fluorescent Ag NCs also showed remarkable selectivity and sensitivity for Hg^{2+} detection due to the strong and specific $Hg^{2+}\cdots Ag^{+}$ interaction. For example, we recently synthesized a highly fluorescent $Ag_{12}(GSH)_{10}$ NC species with a high ratio of active Ag^{+} species on the NC surface (~100%).[106] These blue-emitting Ag NCs exhibited excellent selectivity and sensitivity for Hg^{2+} detection. These examples suggest that controlling the core size of metal NCs is an effective way to construct NC-based fluorometric sensors for environmental pollutants, and the size of metal NCs should be considered while designing a fluorometric sensor.

3.2.2 Core structure matters. Besides the core size, the core structure of metal NCs also affects the fluorescence response of metal NCs upon the introduction of analytes. The core of NCs often consists of several metal atoms, which may feature a closed-shell electronic configuration. It is well-known that the metal cores with a closed-shell electronic configuration (d^{10}) possess high affinity towards other closed-shell metal ions with similar electronic configuration, which can be defined as d^{10}–d^{10} metallophilic interaction.[107,108] Hg^{2+} ion is a closed-shell metal ion with a $5d^{10}$ structure, and both Au(I) and Ag(I) have a similar closed-shell electronic configuration. Therefore, a trace amount of Hg^{2+} could be detected *via* its capability to efficiently quench the fluorescence of Au/Ag NCs due to the formation of a strong metallophilic bond between Hg^{2+} ($5d^{10}$) and Au^{+} ($5d^{10}$)/Ag^{+}($4d^{10}$). We first demonstrated this concept using a red-emitting BSA-Au_{25} NC (~17% of Au^{+} on the surface of Au NCs) to construct a fluorometric sensor for Hg^{2+}, which could efficiently quench the fluorescence of Au NCs owing to the strong metallophilic $Hg^{2+}\cdots Au^{+}$ interaction, as shown in Fig. 5.[109] In a separate study, an NIR Au NC species was synthesized *via* a microwave-reduction protocol,[110] and the as-synthesized NCs showed good performance for the detection of Hg^{2+} in solution. This sensor system can also be used to monitor the concentration of Hg^{2+} inside cancer cells. Another study is to incorporate fluorescent Au NCs into poly(*N*-isopropylacrylamide) (PNIPAM) microgel for the detection of Hg^{2+},[111] where the metallophilic interaction between Au^{+} and Hg^{2+} can significantly quench the fluorescence of Au NCs. Despite a number of successful attempts on the detection of Hg^{2+} based upon metallophilic interaction, the understanding of the underlying chemistry and physics for d^{10}–d^{10} interaction-induced fluorescence quenching is presently lacking. It requires concerted efforts from both experimental and theoretical experts. The above discussions exemplify the importance of the core structure of fluorescent metal NCs in the design of fluorometric sensors for pollutant detection.

3.2.3 Ligand shell matters. The ligand shell may also affect the selectivity and sensitivity of metal NCs because the ligand shell is the first layer that can come into contact with the analytes. A number of ligands (*e.g.*, proteins and thiolates) have been used to prepare fluorescent metal NCs.[112–114] In particular, metal NCs protected by a small organic ligand may feature relatively short diffusion lengths for the analytes, and they can be used to construct good sensors for heavy metal ions. For example, a 11-mercaptoundecanoic acid-protected Au NC species was used to detect Hg^{2+} ions in solution *via* the Hg^{2+}-induced aggregation of Au NCs.[115] However, this approach could not differentiate Hg^{2+} from other multivalent ions such as Pb^{2+} or Cd^{2+}, who have a similar binding affinity with the carboxylic anions as Hg^{2+}. The selectivity

towards Hg^{2+} can be improved by introducing a chelating ligand (*e.g.*, 2,6-pyridinedicarboxylic acid) that can effectively mask the binding ability of Pb^{2+} and Cd^{2+}, but not Hg^{2+}. In a separate study, a poly(methacrylic acid) (PMAA)-protected Ag NC species was used to detect Cu^{2+}, which could effectively quench the fluorescence of Ag NCs in solution.[116] The fluorescence quenching could be attributed to the strong binding between Cu^{2+} and the free carboxylic groups on PMAA. More recently, a label-free method for the "turn-on" detection of Hg^{2+} ions was developed by using DNA duplex stabilized Ag NCs as the fluorescent probe.[117] In the presence of Hg^{2+}, the DNA duplex was strengthened by the formation of a T–Hg^{2+}–T base pair; subsequently, a highly fluorescent Ag NC species was formed due to the sequence-dependent fluorescence property of Ag NCs. Compared to metal NCs protected by small organic ligands, metal NCs protected by proteins are more stable in solution, particularly under harsh conditions, such as under high salt concentrations and oxidative environment. For example, Kawasaki *et al.* synthesized pepsin-protected Au NCs and found that the pH value of the reaction solution was critical for the formation of Au NCs with different sizes such as Au_5, Au_8, Au_{13}, and Au_{25}.[118] The pepsin-Au_{25} NCs were sensitive for the detection of Pb^{2+} *via* the fluorescence enhancement mechanism, and can also be used to detect Hg^{2+} *via* the fluorescence quenching mechanism.

It should be noted that the sensing applications of NMNs are not limited to heavy metal ions. Other common chemicals (*e.g.*, hydrogen peroxide, H_2O_2) and contaminants (*e.g.*, pesticides) can also be detected by the NMNs-based sensors. For example, Guan *et al.* developed an effective process to separate BSA/Au_{25} NCs from free BSA *via* a co-precipitation process with zinc hydroxide. The as-purified NCs exhibited stronger fluorescence in solution and improved sensitivity and selectivity for the fluorescence detection of H_2O_2 (as low as 10 nM) and common pesticides (*e.g.*, dithizone, fenitrothion, paraoxonethyl and 2,4-dichlorophenoxyacetic acid, 1 mM).[119] In another study, Nair *et al.* reported that Au NPs of 10–20 nm can be used for the detection of common pesticide (*e.g.*, endosulfan) in ppm level.[120]

4. Catalytic applications of NMNs

To meet the ever-increasing need of environmental protection and green (environmentally friendly or sustainable) processes, catalytic reactions have been expected to play active roles in the fields of environmental science and materials science.[121] Several recent reviews have highlighted the important advances in fuel cell technology and other energy-related applications using NMNs-based catalysts.[5,21,24,25,43,122] However, the exploration of highly effective NMNs-based catalysts for environmental applications is still in its infancy. Tremendous efforts have been recently devoted to engineer the size, shape, composition, and supports of NMNs. For instance, using a rational combination/integration of engineered NMNs with a pre-designed support, some synergistic effects are expected. In the following section, we will discuss the design of NMNs for heterogeneous catalysis, photocatalysis, and electrocatalysis applications in the field of environment.

4.1 Heterogeneous catalysis

Advanced catalysts often involve noble metals. Among which, Au has attracted an increasing interest due to its unique physicochemical properties and its high selectivity for some catalytic reactions such as the oxidation of hydrocarbon,[123] CO and nitro-compounds,[7] hydrogenations,[124] water-gas shift,[125] hydrochlorination,[126] and propylene epoxidation.[127] Au has rich coordination and organometallic chemistry, but as a catalyst, Au has been considered to be catalytically inert for decades.[21] In 1980s, Haruta and Hutchings independently demonstrated that Au could be a good heterogeneous catalyst. In particular, Haruta *et al.* explored the use of supported Au for CO oxidation at a very low temperature of −70 °C.[128] In addition, Hutchings *et al.* studied the hydrochlorination of acetylene to vinyl chloride using Au as the catalyst.[126] These studies suggest Au can be a promising catalyst for many reactions, and the research on Au catalysis began to flourish.[65,129] Considerable attention has been recently devoted to clarifying the factors that control the activity of Au catalysts, which could provide principles to tailor the catalytic capability of Au catalysts. We will highlight some examples in this section, particularly for the design of Au catalysts for environmental applications.

4.1.1 Size matters. Because the properties of functional materials are highly size dependent, the catalytic activity of Au is also largely dictated by its particle size. In particular, the size of Au NPs determines their surface-to-volume ratios and chemical potentials. A general trend is that the activity of the supported Au catalysts often increases with the decrease of particle size. For example, Zhou *et al.* applied single-molecule fluorescence microscopy to study the catalytic activity of Au NPs and observed the size-dependent activity of Au NPs.[130] In a separate study, Shaikhutdinov *et al.* reported a similar size effect on the adsorption of CO on Au catalysts, where CO could be strongly adsorbed on a smaller sized Au NP.[131] The good catalytic activity of Au catalysts can be attributed to the number of low coordinated Au atoms on the surface of Au NPs. This hypothesis was suggested by a density functional theory (DFT) calculation.[132] More recently, Janssens *et al.* summarized the data of CO oxidation over the past 10 years using Au NPs as the catalyst, where the catalytic activity of Au catalysts at 0 °C was correlated to their particle size.[133] This comprehensive review article clearly suggests that the catalytic activity of supported Au catalysts is highly size dependent. However, some fundamental issues still remain unresolved. For example, the questions such as why Au NPs show high catalytic activity or what is the origin of this high catalytic activity, are still unclear and currently under intense debate among scientists. Some different trends in the size-activity correlation have been reported. For example, Claus *et al.* observed that the catalytic activity and selectivity of the supported Au catalysts increased when the Au NP size increased.[134] To address such

fundamental issues, concerted and continuous efforts are required from both theoretical calculations and experimental development, which may finally provide some insights to uncover the origin of the high activity of Au catalysts.

Recent advances in atomically precise noble metal NCs may provide a good platform to understand these fundamental issues. In particular, the atomically precise metal NCs feature well-defined size, structure, and surface, which could perfectly address some issues in the Au NP system, including the broad size distribution and complicated and unknown surface structures of the NPs. Such issues in Au NPs have largely affected the precise correlation of catalyst structure and electronic properties to their catalytic properties.[50,135] Recently, the ultrasmall and atomically precise Au NCs have rapidly emerged as a new class of Au catalysts with an attractive feature of high selectivity for some catalytic reactions. For example, Valden *et al.* investigated the size dependence of Au NCs (with particle sizes of 1–6 nm, supported on TiO_2) for CO oxidation at a low temperature.[129] They found that the pronounced structure sensitivity of Au/TiO_2 towards CO oxidation originated from the quantum size effects of the Au NCs. As such, the catalytic activity of Au NCs can be well-controlled by adjusting the sizes of the NCs. In another example, Zhu *et al.* systematically studied the catalytic performance of $Au_{25}(SR)_{18}$ NCs towards the selective hydrogenation of α,β-unsaturated ketones and aldehydes to unsaturated alcohols, which achieved a remarkable 100% selectivity.[136] The unique core–shell structure of the $Au_{25}(SR)_{18}$ NCs (Au_{13} core/Au_{12} shell) and their specific electronic structures (electron-rich Au_{13} core and low-coordinate (N = 3) surface Au atoms) are two key factors that may contribute to the superior catalytic performance of Au NCs. The theoretical study also supports that the existence of low coordinated Au atoms on the NC surface was indispensable for H_2 dissociation.[137] Similarly, a more recent study presented an interesting size-dependent catalytic activity of Au for thiophenol oxidation in the presence of O_2, as shown in Fig. 6.[138] The data presented in this study suggest that neither single Au atoms nor Au NPs are catalytically active, but the aggregation of 5–10 Au atoms to form Au clusters showed an activity, which was even higher than sulfhydryl oxidase (a highly active and selective enzyme). Theoretical calculations also suggest that only Au NCs of low atomicity are capable of simultaneously adsorbing and activating thiophenol and O_2, while the larger sized Au NPs are passivated by strongly adsorbed thiolates (RS–Au–SR units).[138] A similar size-dependent catalytic performance of Au NCs was also observed in an immobilized Au_n NC catalyst on hydroxyapatite. This catalyst was used for the selective oxidation of cyclohexane to cyclohexanol and cyclohexanone in the presence of O_2.[14] The turnover frequency (TOF) was monotonically increased as the size increased, with the highest TOF of 18 500 h^{-1} Au $atom^{-1}$ when n = 39; however, this value decreased when the particle size further increased to n = 85. These examples suggest that the size effects of Au catalysts should be considered during the designing of Au NPs or NCs as heterogeneous catalysts for many catalytic reactions.

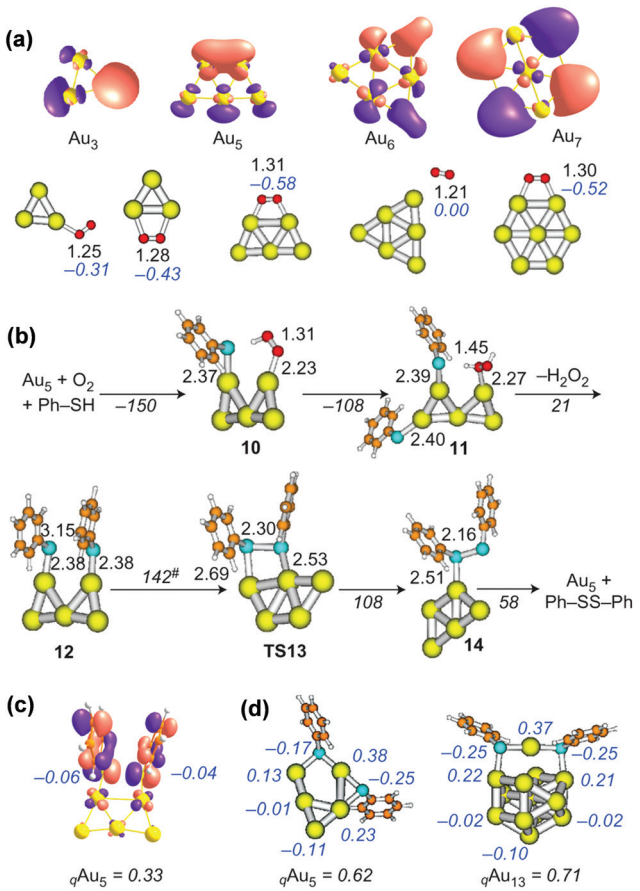

Fig. 6 Reactivity of Au NCs of low atomicity. (a) Atomic distribution of the HOMOs of Au_3, Au_5, Au_6, and Au_7 NCs and the optimized structures of the complexes formed by the interaction of these NCs with O_2. (b) Structures involved in the formation of disulfide catalyzed by Au_5 NC. (c) Atomic distribution of the HOMO of structure 12. (d) Stable linear RS–Au–SR units, or 'staple' motifs, formed over Au_5 and Au_{13} systems. Reprinted with permission from ref. 138. Copyright © 2013 Nature Publishing Group.

4.1.2 Support matters. Considerable emphasis has been placed on the fabrication of high quality catalysts. In particular, the supports could affect the activity and selectivity of the as-fabricated NMNs-based catalysts. Recent studies have shown that TiO_2, Al_2O_3, α-Fe_2O_3, and CeO_2 are good supports, which could be used to host Au catalysts. The effects of oxide supports on the activity and selectivity of Au catalysts have been extensively investigated in past decades. For example, Radnik *et al.* found that the morphology of the Au NPs was greatly influenced by the supports, where more rounded particles were present on TiO_2, while highly faceted particles were observed in the ZnO system. Such morphology differences in different supports could be due to the different Au NP-support interactions.[139] In a separate study, Comotti *et al.* systematically examined the support effects on Au NP catalysis for CO oxidation, and suggested that the best combination is the deposition of Au NPs on TiO_2 and Al_2O_3, which could achieve nearly 100% of CO conversion (ZnO and ZrO_2 hosted Au NPs

showed a considerably lower activity, as shown in Fig. 7).[30] Shimizu *et al.* also reported the size and support dependent catalytic activity of Au NPs for the chemoselective hydrogenation of nitroaromatics.[140] Their data indicated that both small sized Au NPs (*e.g.*, <3 nm) and acid–base bifunctional supports (*e.g.*, Al_2O_3) are indispensable for high catalytic activity. The authors proposed that the cooperation of the acid–base pair sites on Al_2O_3 and the coordinative unsaturated Au atoms on the Au NP surface are crucial for the dissociation of H_2 to yield H^+/H^- pairs at the metal/support interface.

Besides the metal oxide supports, carbon-based materials, such as carbon nanotubes[141] and graphene oxide (GO),[142] can also be used to host the Au NPs for various catalytic applications.[143–145] Among them, the carbon nanotubes are considered as a novel class of promising support materials, which could be complementary to conventional supports. Carbon nanotubes feature remarkable physicochemical properties (*e.g.*, good conductivity and mechanical stability and rich surface chemistry with abundant reactive sites). For example, Castillejos *et al.* used three different technologies—impregnation, organometallic decomposition, and deposition–precipitation—to deposit Au NPs onto pristine and/or nitrogen-doped carbon nanotubes, and evaluated their catalytic activity towards CO oxidation.[143] Their results suggest that the choice of Au precursors, supports, and fabrication chemistry are crucial for controlling the size and location (on or inside the nanotubes) of the Au NPs on carbon nanotubes; such structures dictate the catalytic reactivity of the as-fabricated Au NPs.[146,147]

4.2 Photocatalysis

In a typical photocatalytic system, a photocatalyst is used as a solar-to-fuel converter. Titanium dioxide (TiO_2) is one of the most studied photocatalysts.[148] When TiO_2 absorbs incident light with energy larger than its band gap, electrons and holes are generated in the conduction and valence bands, respectively.[149] However, one of the major limitations for TiO_2 as a photocatalyst is its large band gap of 3.0–3.2 eV, leading to its poor efficiency under visible light. A number of studies have attempted to improve the visible light absorption of TiO_2 by depositing noble metals (*e.g.*, Au, Pt, and Ag), doping with transition metals (*e.g.*, Fe and Zn) and non-metal elements (*e.g.*, N, C, and S), or forming complexes with other narrow band gap semiconductors (*e.g.*, CdS and Cu_2O).[150–154] Among them, the deposition of NMNs on TiO_2 is potentially efficient due to the well-controlled and tunable optical properties of NMNs as well as their excellent photostability.[151,155] The photocatalytic applications of wide band gap semiconductors with the Pt NP deposition have been extensively studied, and the readers may refer to some research and review articles on this topic.[156–158] In this section, the foci will be the effect of size, loading amount, and supports on the photocatalytic activity of Au-doped TiO_2 composites (as an example), highlighting some good designs of photocatalysts with good performance.[21,159]

4.2.1 Size and loading amount matters. Au NPs exhibit a strong visible light absorption due to their unique SPR property.[160] The SPR absorptions of spherical Au NPs are often in the range of 520–550 nm, which could provide the visible light response for some wide band gap semiconductors (*e.g.*, TiO_2). In particular, the conducting electrons of Au NPs will be excited upon illumination, which may directly participate in the redox reactions on the NP surface or migrate to the molecules adsorbed on the supports. The surface barrier between TiO_2 and Au NPs could greatly reduce the chance of the recombination of photogenerated holes and electrons.[161] Silva *et al.* investigated the photocatalytic performance of Au/TiO_2 complex by tuning the excitation wavelength, and they also proposed relevant photocatalytic mechanisms in this study.[162] Under UV light illumination, the electrons from TiO_2 valance band are excited to the conduction band of TiO_2, which subsequently migrate to the surface of Au NPs to participate in the redox reactions, while the photogenerated holes will be quenched by a reducing agent. On the other hand, the excitation of the Au surface plasmon band will generate electron–hole pair upon visible light illumination, and the electrons will be readily transferred to the conducting band of TiO_2.

The successful design of the composite catalysts relies on a thorough understanding of the role of the size of NMNs and the phase of the supports. For example, Murdoch *et al.* reported that Au NPs in the size range of 3–30 nm can greatly enhance the photocatalytic H_2 production rate of both anatase and rutile TiO_2, which by itself is inactive for photocatalytic reactions, as illustrated in Fig. 8.[163] Interestingly, the specific reaction rate of the Au/TiO_2 composite demonstrated size-dependent properties only for Au NPs above 12 nm, and the reaction rate was almost constant for Au NPs in the 3–12 nm range. Various photocatalytic applications of Au/TiO_2, such as photocatalyzed alcohol aerobic oxidation,[164] acetone oxidation,[165] NO oxidation,[166] benzene to phenol oxidation,[167] have been recently explored.

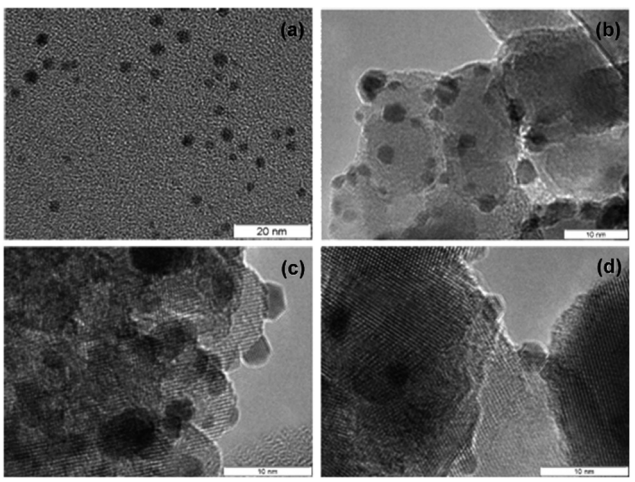

Fig. 7 Representative HRTEM images of (a) Au NPs before deposition and after deposition on (b) ZnO, (c) ZrO_2, and (d) TiO_2. Reprinted with permission from ref. 30. Copyright © 2006 American Chemical Society.

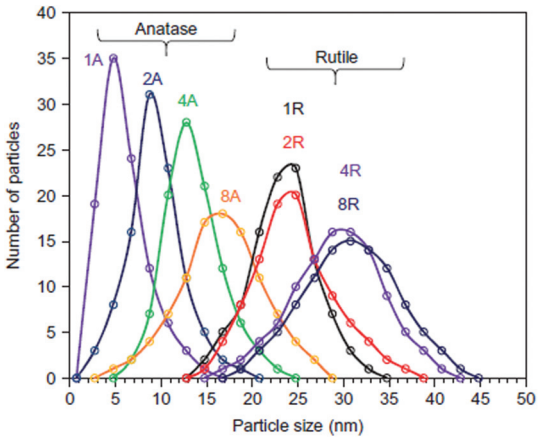

Fig. 8 Particle size distribution of Au on TiO_2 photocatalysts for H_2 production, showing smaller Au particles are present on anatase rather than on rutile. Reprinted with permission from ref. 163. Copyright © 2011 Nature Publishing Group.

Besides the size-dependent activity, the loading amount of Au NPs is also an important factor that could influence the photochemical performance of the Au/TiO_2 nanocomposites. For instance, Li *et al.* applied a novel multicomponent assembly approach to synthesize Au NPs loaded TiO_2 composites and examined their photocatalytic activity by phenol oxidation and chromium-reduction reactions. Their results demonstrated that the photochemical performance of Au/TiO_2 can be efficiently controlled by tailoring the loading ratio of Au NPs, where 0.5 mol% Au was found to be the best.[168] Murdoch *et al.* also demonstrated a loading amount dependent photocatalytic performance for H_2 production.[163] The H_2 production rate increased with Au loading up to 4 wt% onto anatase TiO_2 support, and a further increase in Au loading (to 8 wt%) resulted in a decrease in the reaction rate due to the reduction of the available metal-support sites, where both metal and support are needed for the reaction to occur. Besides working as a high-performance photocatalyst, the Au/TiO_2 composite can also be stimulated by ultrasound. For example, Wang *et al.* reported a novel Au/TiO_2 sono-catalyst with a low Au NPs loading of 0.5 wt%, showing enhanced degradation efficiency for various azo dyes (*e.g.*, orange II, ethyl orange, and acid red G) as compared to pristine TiO_2 and Au nanocatalyst.[169]

When the size of Au NPs further decreases to NC levels, the molecular-like properties become dominant. Previous studies have demonstrated that the HOMO–LUMO excitation behavior of Au NCs led to the formation of absorption peaks in the visible region.[170] More recently, Chen *et al.* found that the GSH-protected Au NCs with tunable absorptions were capable of injecting photogenerated electrons into wide band gap semiconductors (*e.g.*, TiO_2) under simulated solar light illumination. This study suggests Au NCs to be a novel class of photosensitizers.[171,172] In particular, the authors also demonstrated that the mesoscopic TiO_2 films modified with Au NCs exhibited a stable photocurrent density of 3.96 mA cm^{-2} with a power conversion efficiency of 2.3% under AM 1.5 irradiation,[171] and it showed a moderate H_2 production rate of 0.3 mmol h^{-1} g^{-1} photocatalyst under visible light (400–500 nm) illumination.[172] Based on the latest research by Stamplecoskie and Kamat,[173] these GSH-protected Au NCs also exhibited size-dependent excitation states and electron transfer properties. The relatively large sized NCs (*e.g.*, $Au_{25}GSH_{18}$) displayed rapid excitation (<1 ps) as well as slow relaxation (~200 ns), while the smaller counterparts (*e.g.*, $Au_{10-12}GSH_{10-12}$) exhibited only slow relaxation, and the short lifetime relaxation component became less dominant as the size of the Au NCs decreased. Kogo *et al.* also reported the size-dependent electronic structures of Au NCs supported on TiO_2 and estimated the HOMO and LUMO levels of Au NCs based on the photocurrent-irradiation wavelength relationship.[174,175] These Au NCs also demonstrated size-dependent photocatalytic activity, *i.e.*, increase in the photocatalytic reduction yield with decrease in the NC size: Au_{25} < Au_{18} < Au_{15} < Au_{10-12}.

4.2.2 Support matters. As mentioned in the previous section, the support materials also play a significant role in dictating the photocatalytic performance of supported Au catalysts. Besides TiO_2, other semiconductors, such as, CeO_2 [176] and ZnO,[177] also show enhanced photocatalytic activities after Au NP deposition. For example, Ke *et al.* systematically studied the effects of supports (namely, CeO_2, TiO_2, ZrO_2, Al_2O_3, and zeolite Y) on the photocatalytic performance of supported Au NPs, and they found that the Au/CeO_2 photocatalyst evidently demonstrated enhanced photoactivities compared to other counterparts due to its stronger SPR effect and light absorption ability.[178] The phase of the support materials also plays a vital role. It has been reported that the Au NPs of similar size on anatase TiO_2 feature a two orders of magnitude higher rate of H_2 production than that achieved for Au on rutile TiO_2.[163] As for the supported Au NCs, Xiao *et al.* further extended the previous TiO_2 NP film support to a novel TiO_2 nanotube array support.[179] The photochemical performance of the Au NCs decorated TiO_2 nanotube array photoanodes were systematically studied, including the photocatalytic oxidation of organic pollutants (*e.g.*, methyl orange), photocatalytic reduction of aromatic nitro compounds (*e.g.*, nitroaniline), and photoelectrochemical water splitting for H_2 production under simulated solar light irradiation. Similar to the Au NPs supported on semiconductors, the photogenerated electrons of Au NCs under visible light can flow to the conduction band of the semiconductor, while the holes remain at the HOMO of Au NCs for oxidation reactions, enhancing the efficiency of charge separation process.[179] Stamplecoskie *et al.* suggested that the relatively long lifetime of the excited state could make the electron transfer process much easier, for example in the reduction reaction of methyl viologen.[180] Besides Au NCs, the applications of Ag NPs and NCs as photosensitizers were also recently reported.[181,182] These results revealed that the photocatalytic activity of various supported NMNs can be efficiently controlled by fine-tuning the size, support, and other parameters of NMNs.[183]

4.3 Electrocatalysis

Recently, the catalytic activity of NMNs in electrochemical applications has also received extensive research interest. Some important attributes of NMNs that could influence the catalytic activity of NMNs in electrochemical media are morphology, structure, composition, and support, which will be discussed in this section.

4.3.1 Morphology and structure matters. With the evolution of synthetic chemistry, researchers have controlled the morphology and structure of NMNs, which can then be used to further optimize their electrocatalytic activity. Pt-based nanomaterials are the most widely investigated cathode electrocatalysts for the oxygen reduction reaction (ORR). These catalysts are also widely used for anodic electrocatalytic reactions, such as the methanol oxidation reaction (MOR) and ethanol oxidation reaction (EOR). The shape of Pt nanomaterials plays a crucial role in their electrocatalytic performance because the absorption behavior of reactants could be varied on the different facets of the nanocatalysts. For example, Wang *et al.* found that the specific activity of Pt nanocubes for ORR in H_2SO_4 media was considerably higher than that achieved in polyhedrons or truncated cubes possibly because of the different absorption abilities of bi-sulfates on Pt (100) as compared to Pt (111) facets (Fig. 9).[184] In a separate study, Chen *et al.* demonstrated that Pt multi-octahedrons showed better electrocatalytic activity per unit surface area than the commercial catalysts due to a higher ratio of Pt (111) to Pt (100) facets exposed.[185]

Surface structure is also of particular importance for metal electrocatalysts, and high index facets usually exhibit higher activity compared to low index facets, particularly because the atoms located at the edges and steps are catalytically more active. Compared to the commercially available Pt catalysts, the Pt nanostructures with high index facets, namely, (730), (210), and (520), showed 4 and 2 times higher efficiency for formic acid and ethanol electro-oxidation, respectively.[186] Similarly, Au-based electrocatalysts also show remarkable structure sensitivity.[187] Studies on the electrocatalytic activity of Au NPs of various size and surface orientation indicated that the cubic NPs were the most active, while the activity of the nanorod was relatively low.[188,189] Therefore, more strategies should be explored to effectively control the morphology and surface structure of NMNs for electrocatalytic reactions.

4.3.2 Composition matters. In recent decades, the rational design of bi/tri-metallic nanomaterials has attracted particular interest because it could offer unique opportunities to enhance durability as well as reduce the cost of the catalysts. More importantly, these composite nanomaterials often exhibit superior catalytic activity compared to their mono-component counterparts due to the electronic effect and synergistic effect among components. In addition, during the conventional electrochemical processes, some small molecular species (*e.g.*, CO and HCOOH) could adversely adsorb onto the Pt catalyst surface, blocking the active sites and deactivating (or poisoning) the catalyst. Significant efforts have been devoted to exploring Pt-based bimetallic catalysts, such as Pt–Pd, Pt–Ru, and Pt–Au, to further address the poisoning issue. Among them, Pt–Au bimetallic catalysts have received considerable interest because Au nanomaterials can exhibit high catalytic activity toward CO oxidation. For example, Gu *et al.* prepared Pt-decorated Au nanotubes with self-supported high surface area and minimized Pt loading.[190] The as-fabricated alloyed nanostructures possessed enhanced electrocatalytic activity for formic acid oxidation with improved tolerance to CO poisoning. In a separate study, Hong *et al.* developed a bimetallic PdAu nanowire network with an alloyed structure, showing improved activity and stability for ethanol electro-oxidation as compared to commercial Pd/C catalysts in alkaline conditions.[191] Moreover, PdAu nanowires can also serve as a self-supported electrocatalyst without additional supports, thus avoiding the quick loss of electrocatalytic activity, as shown in Fig. 10.

More metal elements can be integrated in one NP to realize a desirable catalytic performance. For example, Cui *et al.* reported the successful synthesis of PdAuCu heterostructured NP catalyst for mixed gas/liquid oxidation.[192] The catalyst took advantage of its unique catalytic activity for H_2O_2 reduction with an over-potential as low as that for ORR. Mazumder *et al.* presented a multi-metallic core–shell structure NP of Pd/Au and Pd/Au/FePt with a constant 5 nm Pd core and controlled shell component and thickness. For this core–shell composite catalyst, an Au shell thinner than 1.5 nm showed a much higher activity than that with 2 nm shell and pure Au.[193] This work demonstrated the controlled catalytic activity of electrocatalysts adjusted by the shell thickness and provided a versatile model of core–shell system for the rational design of high-performance electrocatalyst. Meanwhile, a variety of bi/tri-metallic nanostructures have been synthesized aiming at

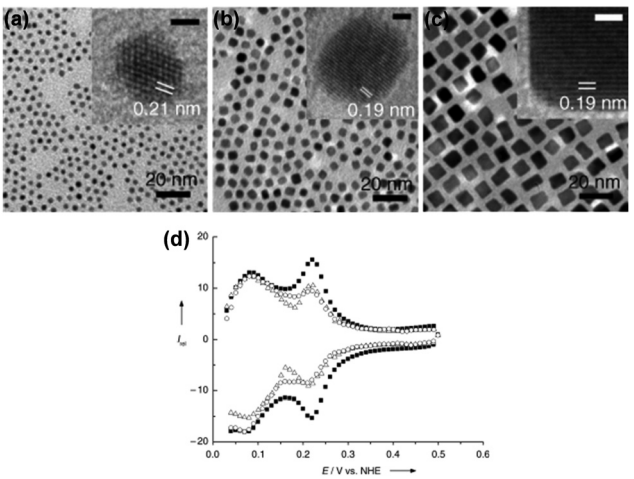

Fig. 9 Representative TEM images of (a) 3 nm polyhedral Pt NP, (b) 5 nm truncated cubic Pt NP, and (c) 7 nm cubic Pt NP. (d) The corresponding cyclic voltammetry curves (○ polyhedron, △ truncated cube, and ■ cube). Reprinted with permission from ref. 184. Copyright © 2008 WILEY-VCH Verlag GmbH & Co. KGaA, Weinheim.

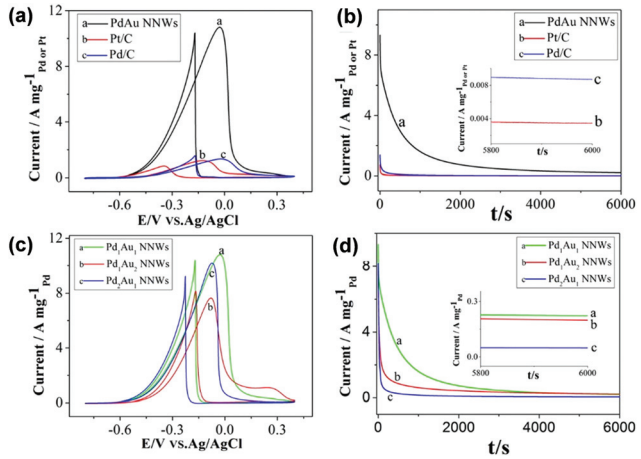

Fig. 10 (a) Mass activity of PdAu nanowires, Pd/C, and Pt/C towards ethanol electrooxidation. (b) Current–time curves of PdAu nanowires, Pd/C, and Pt/C recorded at −0.1 V. (c) Mass activity of PdAu nanowires with different compositions towards ethanol electrooxidation. (d) Current–time curves of PdAu nanowires with different compositions recorded at −0.1 V in a solution containing 1 M ethanol and 1 M potassium hydroxide. Reprinted with permission from ref. 191. Copyright © 2014 American Chemical Society.

decreasing the Pt loading but not sacrificing their activity and durability.[194–198]

4.3.3 Support matters. One important criterion for electrocatalyst design is to maintain its surface area electrochemically active because the catalyst often suffers from aggregation, dissolution, and destruction during the catalytic reactions; these factors may seriously affect the catalytic activity and lifespan of the catalyst.[199,200] One efficient way to mitigate this effect is to design a suitable support material to host the catalyst. The support materials not only possess the dispersion effect, but also modify the electronic property and geometric factor of the catalyst, which in turn could change the catalytic activity and the number of surface active sites. It has been well demonstrated that the high specific surface area, good electronic conductivity, and comparable chemical inertness are the key requirements for an ideal support, which can maximize the electroactive sites of catalyst as well as improve catalytic activity and durability.[201] Carbon blacks are commonly used as catalyst support and many studies have been devoted to uncover the effect of carbon black properties on the electrocatalytic activity of supported catalysts. The carbon supports are usually activated by chemical or physical approaches to increase the anchoring centers for metal catalysts. For example, Yan *et al.* prepared Au NPs supported on activated carbon by a rapid reduction of Au salt on the surface of activated carbon in the presence of polyvinylpyrrolidone (PVP).[202] The specific current density on this catalyst reached 48.6 mA mg^{-1} Au at 0.355 V, showing high activity for ethanol electrooxidation. In addition, other magnetic materials can also be used as support for Au NPs. For example, Hassan *et al.* developed a simple and sensitive biosensor for *Escherichia coli* O157 : H7 detection based on the electrocatalytic property of Au NPs.[203] The superparamagnetic microbeads support was used as a pre-concentration/purification platform with a low LOD of 457 and 309 CFU mL^{-1} in minced beef and tap water, respectively.

More recently, many other alternative carbon materials with versatile nanostructures have been explored for more efficient support materials. Among them, graphene is regarded as the most promising material because its 2D single layer honeycomb structure provides excellent electrical conductivity. Moreover, its ultra-high specific surface area and superior environmental stability makes it an ideal support to host the noble metal catalysts.[204] Graphene supported Pt, Pd, and Au have been explored as electrocatalysts for efficient methanol oxidation[205,206] and ORR.[207,208] For example, Mondal and Jana prepared noble metal (Pt/Pd) graphene nanocomposites, which showed high and stable catalytic current for ethanol and formic acid oxidation.[209] Tiwari *et al.* reported a combination of Pt NCs with double stranded DNA modified GO composite, where the high electrocatalytic performance with enhanced durability could be attributed to the strong interaction between the catalyst and the support, as shown in Fig. 11.[210] Similar phenomena have been observed by Xu and Wu using Au NCs and reduced GO composite.[211] However, a general and comprehensive understanding of the interaction between the support and the catalyst is still lacking, and concerted and continuous efforts are required to uncover the mystery of the support.

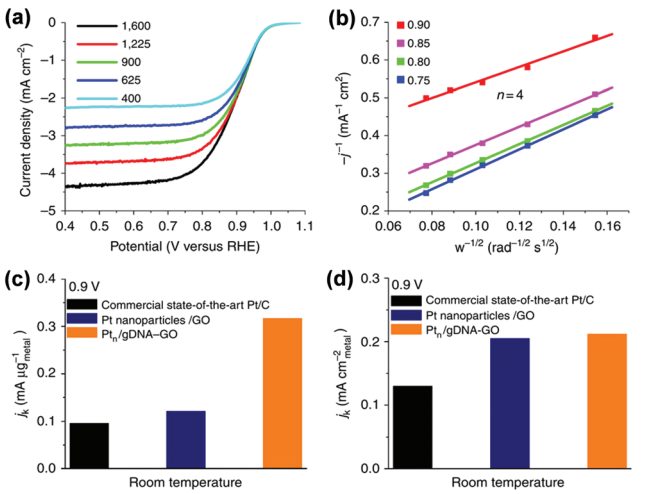

Fig. 11 (a) ORR polarization curves of the Pt_n/gDNA–GO composite in an O_2-saturated 0.1 M $HClO_4$ solution with a sweep rate of 10 mV s^{-1} at different rotation speeds. (b) Corresponding K–L plots at different potentials. (c) Mass activity and (d) specific activity at 0.9 V *versus* reversible hydrogen electrode (RHE) for different catalysts. Mass and specific activities are given as kinetic current densities (j_k) normalized in reference to the loading amount of metal and EASA (EASA from CO stripping), respectively. Reprinted with permission from ref. 210. Copyright © 2013 Nature Publishing Group.

5. Conclusions

The unique physicochemical properties of NMNs, in combination with their well-controlled and tunable structural parameters (*e.g.*, size, shape, composition, and surface), have made them good platforms for various environmental applications. Recent advances in the preparation and characterization of well-defined NMNs have facilitated the preparation of more efficient environmental sensors and catalysts. Moreover, some fundamental studies on NMNs, such as elucidating the micro-structure and identifying the catalytically active sites, also provide better understanding of the rational design of NMNs.

By tailoring the size/shape, composition, surface/support, and other parameters/attributes of NMNs, one can fine-tune the physicochemical properties of NMNs for various environmental applications. In general, the NMNs-based environmental sensors are attractive to the community due to their simple construction and operation as well as good performance, especially when combined with some emerging micro/nano-array technologies. Nevertheless, the development of highly sensitive and selective sensors for the analysis of complicated environmental samples is still lacking, and a number of key challenging issues need to be overcome. In addition, more efforts are required to widen the detection spectrum, and to improve the selectivity and sensitivity towards real samples in different matrices.

Some other limitations also need to be addressed. For environmental catalytic applications, the need for highly active NMN-based catalysts has spurred intensive interest not only in developing high-quality NMNs with well-controlled and tunable size, morphology, structure, and composition, but also in the rational combination and integration of NMNs-based catalyst into various supporting materials (often to realize synergistic effects). Recent advances in NMNs with well-defined structures (such as ultra-small metal NCs) provide a good opportunity for engineering their catalytic properties for various environmental applications. However, some fundamental issues still remain unresolved such as how the size, surface structure, composition, and support materials affect the catalytic properties of NMNs. Furthermore, other fundamental issues on the active sites and their evolution during the catalytic reactions, as well as the interactions between the NMNs and supports also require concerted efforts from the community.

Acknowledgements

The authors acknowledge the financial support from Singapore National Research Foundation under its Environment and Water Technologies Strategic Research Programme, administered by the Environment and Water Industry Programme Office (EWI) of the PUB on projects 1102-IRIS-11-01 (NUS grant number of R-279-000-381-279) and 1102-IRIS-14-03 (NUS grant number of R-706-000-025-279); T. Chen acknowledges the National University of Singapore for his research scholarship. Y. Liu and J. Xie also thank the GE-NERI grant support (GE-NERI2014, grant number R-706-005-004-592).

Notes and references

1 Y. Teng, J. Yang, R. Zuo and J. Wang, *J. Earth Sci.*, 2011, **22**, 658.
2 C. C. Mayorga-Martinez, F. Pino, S. Kurbanoglu, L. Rivas, S. A. Ozkan and A. Merkoçi, *J. Mater. Chem. B*, 2014, **2**, 2233.
3 M. M. Huber, S. Canonica, G. Y. Park and U. Von Gunten, *Environ. Sci. Technol.*, 2003, **37**, 1016.
4 L. F. Greenlee, D. F. Lawler, B. D. Freeman, B. Marrot and P. Moulin, *Water Res.*, 2009, **43**, 2317.
5 S. Guo and E. Wang, *Nano Today*, 2011, **6**, 240.
6 Y. Cao, D. Li, F. Jiang, Y. Yang and Z. Huang, *J. Nanomater.*, 2013, **2013**, 123812.
7 A. Corma and P. Serna, *Science*, 2006, **313**, 332.
8 F. Qu, N. B. Li and H. Q. Luo, *J. Phys. Chem. C*, 2013, **117**, 3548.
9 B. R. Cuenya, *Thin Solid Films*, 2010, **518**, 3127.
10 Q. Zhang, J. Xie, Y. Yu, J. Yang and J. Y. Lee, *Small*, 2010, **6**, 523.
11 S. Zeng, D. Baillargeat, H. P. Ho and K. T. Yong, *Chem. Soc. Rev.*, 2014, **43**, 3426.
12 M. Daniel and D. Astruc, *Chem. Rev.*, 2004, **104**, 293.
13 P. Rodriguez, Y. Kwon and M. T. Koper, *Nat. Chem.*, 2012, **4**, 177.
14 Y. Liu, H. Tsunoyama, T. Akita, S. Xie and T. Tsukuda, *ACS Catal.*, 2011, **1**, 2.
15 M. D. Hughes, Y. J. Xu, P. Jenkins, P. McMorn, P. Landon, D. I. Enache, A. F. Carley, G. A. Attard, G. J. Hutchings, F. King, E. H. Stitt, P. Johnston, K. Griffin and C. J. Kiely, *Nature*, 2005, **437**, 1132.
16 T. Pradeep and Anshup, *Thin Solid Films*, 2009, **517**, 6441.
17 N. V. Long, Y. Yang, C. Minh Thi, N. V. Minh, Y. Cao and M. Nogami, *Nano Energy*, 2013, **2**, 636.
18 E. Roduner, *Chem. Soc. Rev.*, 2006, **35**, 583.
19 L. B. Zhang and E. K. Wang, *Nano Today*, 2014, **9**, 132.
20 J. Du, B. Zhu, X. Peng and X. Chen, *Small*, 2014, **10**, 3461.
21 A. S. Hashmi and G. J. Hutchings, *Angew. Chem., Int. Ed.*, 2006, **45**, 7896.
22 Z. T. Luo, K. Y. Zheng and J. P. Xie, *Chem. Commun.*, 2014, **50**, 5143.
23 C. Y. Tay, M. I. Setyawati, J. Xie, W. J. Parak and D. T. Leong, *Adv. Funct. Mater.*, 2014, **24**, 5936.
24 B. Wu and N. Zheng, *Nano Today*, 2013, **8**, 168.
25 C. H. Cui and S. H. Yu, *Acc. Chem. Res.*, 2013, **46**, 1427.
26 Y. Sun and Y. Xia, *Science*, 2002, **298**, 2176.
27 Y. Tang and M. Ouyang, *Nat. Mater.*, 2007, **6**, 754.
28 N. R. Jana, L. Gearheart and C. J. Murphy, *J. Phys. Chem. B*, 2001, **105**, 4065.
29 P. Kundu, U. Chandni, A. Ghosh and N. Ravishankar, *Nanoscale*, 2012, **4**, 433.

30 M. Comotti, W. C. Li, B. Spliethoff and F. Schuth, *J. Am. Chem. Soc.*, 2006, **128**, 917.
31 H. Liu and Q. Yang, *CrystEngComm*, 2011, **13**, 2281.
32 N. Zhao, Y. Wei, N. Sun, Q. Chen, J. Bai, L. Zhou, Y. Qin, M. Li and L. Qi, *Langmuir*, 2008, **24**, 991.
33 J. Xiao and L. Qi, *Nanoscale*, 2011, **3**, 1383.
34 S. E. Skrabalak, J. Chen, Y. Sun, X. Lu, L. Au, C. M. Cobley and Y. Xia, *Acc. Chem. Res.*, 2008, **41**, 1587.
35 J. Xie, J. Y. Lee, D. I. C. Wang and Y. P. Ting, *ACS Nano*, 2007, **1**, 429.
36 S. K. Das, A. R. Das and A. K. Guha, *Small*, 2010, **6**, 1012.
37 S. K. Das, A. R. Das and A. K. Guha, *Langmuir*, 2009, **25**, 8192.
38 S. K. Das, M. M. R. Khan, A. K. Guha, A. R. Das and A. B. Mandal, *Bioresour. Technol.*, 2012, **124**, 495.
39 S. K. Das, M. M. R. Khan, T. Parandhaman, F. Laffir, A. K. Guha, G. Sekaran and A. B. Mandal, *Nanoscale*, 2013, **5**, 5549.
40 M. Brust, M. Walker, D. Bethell, D. J. Schiffrin and R. Whyman, *J. Chem. Soc., Chem. Commun.*, 1994, 801.
41 I. Chakraborty, S. Bag, U. Landman and T. Pradeep, *J. Phys. Chem. Lett.*, 2013, **4**, 2769.
42 C. Zeng, C. Liu, Y. Chen, N. L. Rosi and R. Jin, *J. Am. Chem. Soc.*, 2014, **136**, 11922.
43 X. Tan and R. Jin, *WIREs Nanomed. Nanobiotechnol.*, 2013, **5**, 569.
44 G. Schmid and D. Fenske, *Philos. Trans. R. Soc., A.*, 2010, **368**, 1207.
45 Q. Yao, X. Yuan, Y. Yu, Y. Yu, J. Xie and J. Y. Lee, *J. Am. Chem. Soc.*, 2015, **137**, 2128.
46 X. D. Zhang, Z. Luo, J. Chen, X. Shen, S. Song, Y. Sun, S. Fan, F. Fan, D. T. Leong and J. Xie, *Adv. Mater.*, 2014, **26**, 4565.
47 X. Yuan, B. Zhang, Z. Luo, Q. Yao, D. T. Leong, N. Yan and J. Xie, *Angew. Chem., Int. Ed.*, 2014, **53**, 4623.
48 H. Qian, M. Zhu, Z. Wu and R. Jin, *Acc. Chem. Res.*, 2012, **45**, 1470.
49 Z. Wu, E. Lanni, W. Chen, M. E. Bier, D. Ly and R. Jin, *J. Am. Chem. Soc.*, 2009, **131**, 16672.
50 S. Yamazoe, K. Koyasu and T. Tsukuda, *Acc. Chem. Res.*, 2014, **47**, 816.
51 P. Maity, S. Xie, M. Yamauchi and T. Tsukuda, *Nanoscale*, 2012, **4**, 4027.
52 Y. Niihori, W. Kurashige, M. Matsuzaki and Y. Negishi, *Nanoscale*, 2013, **5**, 508.
53 W. Kurashige, Y. Niihori, S. Sharma and Y. Negishi, *J. Phys. Chem. Lett.*, 2014, **5**, 4134.
54 T. U. B. Rao, B. Nataraju and T. Pradeep, *J. Am. Chem. Soc.*, 2010, **132**, 16304.
55 X. Yuan, M. I. Setyawati, A. S. Tan, C. N. Ong, D. T. Leong and J. Xie, *NPG Asia Mater.*, 2013, **5**, e39.
56 Y. Yu, X. Chen, Q. Yao, Y. Yu, N. Yan and J. Xie, *Chem. Mater.*, 2013, **25**, 946.
57 Y. Yu, Z. Luo, Y. Yu, J. Y. Lee and J. Xie, *ACS Nano*, 2012, **6**, 7920.
58 A. Desireddy, B. E. Conn, J. Guo, B. Yoon, R. N. Barnett, B. M. Monahan, K. Kirschbaum, W. P. Griffith, R. L. Whetten, U. Landman and T. P. Bigioni, *Nature*, 2013, **501**, 399.
59 B. Yoon, W. D. Luedtke, R. N. Barnett, J. Gao, A. Desireddy, B. E. Conn, T. Bigioni and U. Landman, *Nat. Mater.*, 2014, **13**, 807.
60 L. Shang, S. Dong and G. U. Nienhaus, *Nano Today*, 2011, **6**, 401.
61 Q. Yao, Y. Yu, X. Yuan, Y. Yu, D. Zhao, J. Xie and J. Y. Lee, *Angew. Chem., Int. Ed.*, 2015, **54**, 184.
62 Z. Luo, V. Nachammai, B. Zhang, N. Yan, D. T. Leong, D. E. Jiang and J. Xie, *J. Am. Chem. Soc.*, 2014, **136**, 10577.
63 X. Dou, X. Yuan, Y. Yu, Z. Luo, Q. Yao, D. T. Leong and J. Xie, *Nanoscale*, 2014, **6**, 157.
64 Y. Yu, Q. Zhang, J. Xie and J. Y. Lee, *Nat. Commun.*, 2013, **4**, 1454.
65 S. Link and M. A. El-Sayed, *J. Phys. Chem. B*, 1999, **103**, 4212.
66 C. I. Richards, S. Choi, J. C. Hsiang, Y. Antoku, T. Vosch, A. Bongiorno, Y. L. Tzeng and R. M. Dickson, *J. Am. Chem. Soc.*, 2008, **130**, 5038.
67 X. Y. Dou, X. Yuan, Q. F. Yao, Z. T. Luo, K. Y. Zheng and J. P. Xie, *Chem. Commun.*, 2014, **50**, 7459.
68 J. Jung, S. Kang and Y. K. Han, *Nanoscale*, 2012, **4**, 4206.
69 X. Yuan, Z. Luo, Y. Yu, Q. Yao and J. Xie, *Chem. – Asian J.*, 2013, **8**, 858.
70 P. K. Jain, X. Huang, I. H. El-Sayed and M. A. El-Sayed, *Acc. Chem. Res.*, 2008, **41**, 1578.
71 G. B. Shan, R. Y. Surampalli, R. D. Tyagi and T. C. Zhang, *Front. Environ. Sci. Eng.*, 2009, **3**, 249.
72 B. Pandey and M. H. Fulekar, *Res. J. Chem. Sci.*, 2012, **2**, 90.
73 M. I. Setyawati, W. Fang, S. L. Chia and D. T. Leong, *Asia-Pac. J. Chem. Eng.*, 2013, **8**, 205.
74 G. Aragay, J. Pons and A. Merkoçi, *Chem. Rev.*, 2011, **111**, 3433.
75 K. Saha, S. S. Agasti, C. Kim, X. N. Li and V. M. Rotello, *Chem. Rev.*, 2012, **112**, 2739.
76 P. C. Chen, P. Roy, L. Y. Chen, R. Ravindranath and H. T. Chang, *Part. Part. Syst. Char.*, 2014, **31**, 917.
77 S. Yoon, E. W. Miller, Q. He, P. H. Do and C. J. Chang, *Angew. Chem., Int. Ed.*, 2007, **46**, 6658.
78 L. Zeng, E. W. Miller, A. Pralle, E. Y. Isacoff and C. J. Chang, *J. Am. Chem. Soc.*, 2005, **128**, 10.
79 L. Basabe-Desmonts, D. N. Reinhoudt and M. Crego-Calama, *Chem. Soc. Rev.*, 2007, **36**, 993.
80 P. C. Ray, *Chem. Rev.*, 2010, **110**, 5332.
81 R. Wilson, *Chem. Soc. Rev.*, 2008, **37**, 2028.
82 H. Choi, C. Baik, S. O. Kang, J. Ko, M.-S. Kang, M. K. Nazeeruddin and M. Grätzel, *Angew. Chem., Int. Ed.*, 2008, **120**, 333.
83 M. L. Juan, M. Righini and R. Quidant, *Nat. Photonics*, 2011, **5**, 349.
84 P. K. Jain, K. S. Lee, I. H. El-Sayed and M. A. El-Sayed, *J. Phys. Chem. B*, 2006, **110**, 7238.

85 F. Chai, C. Wang, T. Wang, L. Li and Z. Su, *ACS Appl. Mater. Interfaces*, 2010, **2**, 1466.
86 X. Liu, M. Atwater, J. Wang and Q. Huo, *Colloids Surf., B*, 2007, **58**, 3.
87 D. Liu, W. Qu, W. Chen, W. Zhang, Z. Wang and X. Jiang, *Anal. Chem.*, 2010, **82**, 9606.
88 K. P. Lisha, Anshup and T. Pradeep, *Gold Bull.*, 2009, **42**, 144.
89 Y. H. Chien, C. C. Huang, S. W. Wang and C. S. Yeh, *Green Chem.*, 2011, **13**, 1162.
90 H. K. Sung, S. Y. Oh, C. Park and Y. Kim, *Langmuir*, 2013, **29**, 8978.
91 Y. L. Hung, T. M. Hsiung, Y. Y. Chen, Y. F. Huang and C. C. Huang, *J. Phys. Chem. C*, 2010, **114**, 16329.
92 J. Yguerabide and E. E. Yguerabide, *Anal. Biochem.*, 1998, **262**, 137.
93 Y. Wang, F. Yang and X. Yang, *ACS Appl. Mater. Interfaces*, 2010, **2**, 339.
94 G. W. Wu, S. B. He, H. P. Peng, H. H. Deng, A. L. Liu, X. H. Lin, X. H. Xia and W. Chen, *Anal. Chem.*, 2014, **86**, 10955.
95 G. Sener, L. Uzun and A. Denizli, *Anal. Chem.*, 2014, **86**, 514.
96 J. M. Slocik, J. S. Zabinski, D. M. Phillips and R. R. Naik, *Small*, 2008, **4**, 548.
97 J. S. Lee, M. S. Han and C. A. Mirkin, *Angew. Chem., Int. Ed.*, 2007, **46**, 4093.
98 X. Xue, F. Wang and X. Liu, *J. Am. Chem. Soc.*, 2008, **130**, 3244.
99 S. Choi, R. M. Dickson and J. H. Yu, *Chem. Soc. Rev.*, 2012, **41**, 1867.
100 J. Zheng, P. R. Nicovich and R. M. Dickson, *Annu. Rev. Phys. Chem.*, 2007, **58**, 409.
101 Y. Lu and W. Chen, *Chem. Soc. Rev.*, 2012, **41**, 3594.
102 J. Zheng, C. W. Zhang and R. M. Dickson, *Phys. Rev. Lett.*, 2004, **93**, 077402.
103 Z. K. Wu, M. Wang, J. Yang, X. H. Zheng, W. P. Cai, G. W. Meng, H. F. Qian, H. M. Wang and R. C. Jin, *Small*, 2012, **8**, 2028.
104 Y. H. Lin and W. L. Tseng, *Anal. Chem.*, 2010, **82**, 9194.
105 Y. Yue, T. Y. Liu, H. W. Li, Z. Liu and Y. Wu, *Nanoscale*, 2012, **4**, 2251.
106 X. Yuan, T. J. Yeow, Q. Zhang, J. Y. Lee and J. Xie, *Nanoscale*, 2012, **4**, 1968.
107 P. Pyykko, *Angew. Chem., Int. Ed.*, 2004, **43**, 4412.
108 N. Goswami, A. Giri, S. Kar, M. S. Bootharaju, R. John, P. L. Xavier, T. Pradeep and S. K. Pal, *Small*, 2012, **8**, 3175.
109 J. Xie, Y. Zheng and J. Y. Ying, *Chem. Commun.*, 2010, **46**, 961.
110 L. Shang, L. Yang, F. Stockmar, R. Popescu, V. Trouillet, M. Bruns, D. Gerthsen and G. U. Nienhaus, *Nanoscale*, 2012, **4**, 4155.
111 L. Y. Chen, C. M. Ou, W. Y. Chen, C. C. Huang and H. T. Chang, *ACS Appl. Mater. Interfaces*, 2013, **5**, 4383.
112 R. Jin, *Nanoscale*, 2010, **2**, 343.
113 I. Diez and R. H. A. Ras, *Nanoscale*, 2011, **3**, 1963.
114 D. M. Chevrier, A. Chatt and P. Zhang, *J. Nanophotonics*, 2012, **6**, 064504.
115 C. C. Huang, Z. Yang, K. H. Lee and H. T. Chang, *Angew. Chem., Int. Ed.*, 2007, **46**, 6824.
116 L. Shang and S. Dong, *J. Mater. Chem.*, 2008, **18**, 4636.
117 L. Deng, Z. Zhou, J. Li, T. Li and S. Dong, *Chem. Commun.*, 2011, **47**, 11065.
118 H. Kawasaki, K. Hamaguchi, I. Osaka and R. Arakawa, *Adv. Funct. Mater.*, 2011, **21**, 3508.
119 G. Guan, S. Y. Zhang, Y. Cai, S. Liu, M. S. Bharathi, M. Low, Y. Yu, J. Xie, Y. Zheng, Y. W. Zhang and M. Y. Han, *Chem. Commun.*, 2014, **50**, 5703.
120 A. Sreekumaran Nair, R. T. Tom and T. Pradeep, *J. Environ. Monit.*, 2003, **5**, 363.
121 N. Yan, *Nanotechnol. Rev.*, 2013, **2**, 485.
122 H. Li, L. Li and Y. Li, *Nanotechnol. Rev.*, 2013, **2**, 515.
123 H. Tsunoyama, N. Ichikun, H. Sakurai and T. Tsukuda, *J. Am. Chem. Soc.*, 2009, **131**, 7086.
124 M. Haruta, *Nature*, 2005, **437**, 1098.
125 Q. Fu, H. Saltsburg and M. Flytzani-Stephanopoulos, *Science*, 2003, **301**, 935.
126 G. J. Hutchings, *J. Catal.*, 1985, **96**, 292.
127 S. Lee, L. M. Molina, M. J. Lopez, J. A. Alonso, B. Hammer, B. Lee, S. Seifert, R. E. Winans, J. W. Elam, M. J. Pellin and S. Vajda, *Angew. Chem., Int. Ed.*, 2009, **48**, 1467.
128 M. Haruta, T. Kobayashi, H. Sano and N. Yamada, *Chem. Lett.*, 1987, **16**, 405.
129 M. Valden, X. Lai and D. W. Goodman, *Science*, 1998, **281**, 1647.
130 X. Zhou, W. Xu, G. Liu, D. Panda and P. Chen, *J. Am. Chem. Soc.*, 2010, **132**, 138.
131 S. K. Shaikhutdinov, R. Meyer, M. Naschitzki, M. Bäumer and H. J. Freund, *Catal. Lett.*, 2003, **86**, 211.
132 N. Lopez and J. K. Nørskov, *J. Am. Chem. Soc.*, 2002, **124**, 11262.
133 T. V. W. Janssens, B. S. Clausen, B. Hvolbæk, H. Falsig, C. H. Christensen, T. Bligaard and J. K. Nørskov, *Top. Catal.*, 2007, **44**, 15.
134 P. Claus, A. Bruckner, C. Mohr and H. Hofmeister, *J. Am. Chem. Soc.*, 2000, **122**, 11430.
135 X. Nie, H. Qian, Q. Ge, H. Xu and R. Jin, *ACS Nano*, 2012, **6**, 6014.
136 Y. Zhu, H. Qian, B. A. Drake and R. Jin, *Angew. Chem., Int. Ed.*, 2010, **49**, 1295.
137 A. Corma, M. Boronat, S. González and F. Illas, *Chem. Commun.*, 2007, 3371.
138 A. Corma, P. Concepcion, M. Boronat, M. J. Sabater, J. Navas, M. J. Yacaman, E. Larios, A. Posadas, M. A. Lopez-Quintela, D. Buceta, E. Mendoza, G. Guilera and A. Mayoral, *Nat. Chem.*, 2013, **5**, 775.
139 J. Radnik, C. Mohr and P. Claus, *Phys. Chem. Chem. Phys.*, 2003, **5**, 172.
140 K. Shimizu, Y. Miyamoto, T. Kawasaki, T. Tanji, Y. Tai and A. Satsuma, *J. Phys. Chem. C*, 2009, **113**, 17803.

141 B. Li, P. He, G. Yi, H. Lin and Y. Yuan, *Catal. Lett.*, 2009, **133**, 33.
142 L. Shao, X. Huang, D. Teschner and W. Zhang, *ACS Catal.*, 2014, **4**, 2369.
143 E. Castillejos, R. Chico, R. Bacsa, S. Coco, P. Espinet, M. Pérez-Cadenas, A. Guerrero-Ruiz, I. Rodríguez-Ramos and P. Serp, *Eur. J. Inorg. Chem.*, 2010, **2010**, 5096.
144 E. G. Rodrigues, S. A. C. Carabineiro, J. J. Delgado, X. Chen, M. F. R. Pereira and J. J. M. Órfão, *J. Catal.*, 2012, **285**, 83.
145 A. Chen, J. Qi, Q. Zhao, Y. Li, G. Zhang, F. Zhang and X. Fan, *RSC Adv.*, 2013, **3**, 8973.
146 N. Zheng and G. D. Stucky, *J. Am. Chem. Soc.*, 2006, **128**, 14278.
147 L. Alves, B. Ballesteros, M. Boronat, J. R. Cabrero-Antonino, P. Concepcion, A. Corma, M. A. Correa-Duarte and E. Mendoza, *J. Am. Chem. Soc.*, 2011, **133**, 10251.
148 Y. Ma, X. Wang, Y. Jia, X. Chen, H. Han and C. Li, *Chem. Rev.*, 2014, **114**, 9987.
149 A. Fujishima, T. N. Rao and D. A. Tryk, *J. Photochem. Photobiol., C*, 2000, **1**, 1.
150 D. Mitoraj and H. Kisch, *Angew. Chem., Int. Ed.*, 2008, **47**, 9975.
151 Z. Liu, W. Hou, P. Pavaskar, M. Aykol and S. B. Cronin, *Nano Lett.*, 2011, **11**, 1111.
152 Y. Liu, H. Zhou, B. Zhou, J. Li, H. Chen and W. Cai, *Nano-Micro Lett.*, 2011, **62**, 2783.
153 S. U. M. Khan, *Science*, 2002, **297**, 2243.
154 Y. Liu, H. Zhou, B. Zhou, J. Li, H. Chen, J. Wang, J. Bai, W. Shangguan and W. Cai, *Int. J. Hydrogen Energy*, 2011, **36**, 167.
155 Y. Tian and T. Tatsuma, *J. Am. Chem. Soc.*, 2005, **127**, 7632.
156 O. Rosseler, M. V. Shankar, M. K. Du, L. Schmidlin, N. Keller and V. Keller, *J. Catal.*, 2010, **269**, 179.
157 J. G. Yu, L. F. Qi and M. Jaroniec, *J. Phys. Chem. C*, 2010, **114**, 13118.
158 Y. Shiraishi, Y. Sugano, S. Tanaka and T. Hirai, *Angew. Chem., Int. Ed.*, 2010, **49**, 1656.
159 A. Corma and H. Garcia, *Chem. Soc. Rev.*, 2008, **37**, 2096.
160 C. J. Orendorff, T. K. Sau and C. J. Murphy, *Small*, 2006, **2**, 636.
161 A. Primo, A. Corma and H. Garcia, *Phys. Chem. Chem. Phys.*, 2011, **13**, 886.
162 C. G. Silva, R. Juarez, T. Marino, R. Molinari and H. Garcia, *J. Am. Chem. Soc.*, 2011, **133**, 595.
163 M. Murdoch, G. I. N. Waterhouse, M. A. Nadeem, J. B. Metson, M. A. Keane, R. F. Howe, J. Llorca and H. Idriss, *Nat. Chem.*, 2011, **3**, 489.
164 D. Tsukamoto, Y. Shiraishi, Y. Sugano, S. Ichikawa, S. Tanaka and T. Hirai, *J. Am. Chem. Soc.*, 2012, **134**, 6309.
165 L. Liu, S. Ouyang and J. Ye, *Angew. Chem., Int. Ed.*, 2013, **52**, 6689.
166 D. Zhang, M. Wen, S. Zhang, P. Liu, W. Zhu, G. Li and H. Li, *Appl. Catal., B*, 2014, **147**, 610.
167 Z. Zheng, B. Huang, X. Qin, X. Zhang, Y. Dai and M.-H. Whangbo, *J. Mater. Chem.*, 2011, **21**, 9079.
168 H. Li, Z. Bian, J. Zhu, Y. Huo, H. Li and Y. Lu, *J. Am. Chem. Soc.*, 2007, **129**, 4538.
169 Y. Wang, D. Zhao, W. Ma, C. Chen and J. Zhao, *Environ. Sci. Technol.*, 2008, **42**, 6173.
170 M. Zhu, C. M. Aikens, F. J. Hollander, G. C. Schatz and R. Jin, *J. Am. Chem. Soc.*, 2008, **130**, 5883.
171 Y. S. Chen, H. Choi and P. V. Kamat, *J. Am. Chem. Soc.*, 2013, **135**, 8822.
172 Y. S. Chen and P. V. Kamat, *J. Am. Chem. Soc.*, 2014, **136**, 6075.
173 K. G. Stamplecoskie and P. V. Kamat, *J. Am. Chem. Soc.*, 2014, **136**, 11093.
174 A. Kogo, N. Sakai and T. Tatsuma, *Nanoscale*, 2012, **4**, 4217.
175 N. Sakai and T. Tatsuma, *Adv. Mater.*, 2010, **22**, 3185.
176 A. Primo, T. Marino, A. Corma, R. Molinari and H. Garcia, *J. Am. Chem. Soc.*, 2011, **133**, 6930.
177 T. H. Yang, L. D. Huang, Y. W. Harn, C. C. Lin, J. K. Chang, C. I. Wu and J. M. Wu, *Small*, 2013, **9**, 3169.
178 X. Ke, X. Zhang, J. Zhao, S. Sarina, J. Barry and H. Zhu, *Green Chem.*, 2013, **15**, 236.
179 F. X. Xiao, S. F. Hung, J. Miao, H. Y. Wang, H. Yang and B. Liu, *Small*, 2015, **11**, 554.
180 K. G. Stamplecoskie, Y. S. Chen and P. V. Kamat, *J. Phys. Chem. C*, 2014, **118**, 1370.
181 S. K. Bhunia and N. R. Jana, *ACS Appl. Mater. Interfaces*, 2014, **6**, 20085.
182 N. Sakai, S. Nakamura and T. Tatsuma, *Dalton Trans.*, 2013, **42**, 16162.
183 J. Zhang, H. Chen, H. Li, J. Di, M. Chen, F. Geng, Z. Zhao and Q. Li, *Chem. Mater.*, 2014, **26**, 2789.
184 C. Wang, H. Daimon, T. Onodera, T. Koda and S. Sun, *Angew. Chem., Int. Ed.*, 2008, **47**, 3588.
185 J. Chen, B. Lim, E. P. Lee and Y. Xia, *Nano Today*, 2009, **4**, 81.
186 N. Tian, Z. Y. Zhou, S. G. Sun, Y. Ding and Z. L. Wang, *Science*, 2007, **316**, 732.
187 P. Rodriguez, N. Garcia-Araez, A. Koverga, S. Frank and M. T. M. Koper, *Langmuir*, 2010, **26**, 12425.
188 J. J. Feng, A. Q. Li, Z. Lei and A. J. Wang, *ACS Appl. Mater. Interfaces*, 2012, **4**, 2570.
189 B. Ballarin, M. C. Cassani, C. Maccato and A. Gasparotto, *Nanotechnology*, 2011, **22**, 275711.
190 X. Gu, X. Cong and Y. Ding, *ChemPhysChem*, 2010, **11**, 841.
191 W. Hong, J. Wang and E. Wang, *ACS Appl. Mater. Interfaces*, 2014, **6**, 9481.
192 C. H. Cui, H. H. Li, J. W. Yu, M. R. Gao and S. H. Yu, *Angew. Chem., Int. Ed.*, 2010, **49**, 9149.
193 V. Mazumder, M. Chi, K. L. More and S. Sun, *Angew. Chem., Int. Ed.*, 2010, **49**, 9368.
194 L. Chen, L. Kuai, X. Yu, W. Li and B. Geng, *Chem. – Eur. J.*, 2013, **19**, 11753.

195 M. Chen, B. Wu, J. Yang and N. Zheng, *Adv. Mater.*, 2012, **24**, 862.
196 C. H. Cui, J. W. Yu, H. H. Li, M. R. Gao, H. W. Liang and S. H. Yu, *ACS Nano*, 2011, **5**, 4211.
197 Y. Y. Feng, Z. H. Liu, Y. Xu, P. Wang, W. H. Wang and D. S. Kong, *J. Power Sources*, 2013, **232**, 99.
198 J. W. Hong, D. Kim, Y. W. Lee, M. Kim, S. W. Kang and S. W. Han, *Angew. Chem., Int. Ed.*, 2011, **50**, 8876.
199 V. Radmilovic, H. A. Gasteiger and P. N. Ross, *J. Catal.*, 1995, **154**, 98.
200 E. Antolini, *Appl. Catal., B*, 2009, **88**, 1.
201 J. C. Meier, C. Galeano, I. Katsounaros, J. Witte, H. J. Bongard, A. A. Topalov, C. Baldizzone, S. Mezzavilla, F. Schuth and K. J. Mayrhofer, *Beilstein J. Nanotechnol.*, 2014, **5**, 44.
202 S. Yan, S. Zhang, Y. Lin and G. Liu, *J. Phys. Chem. C*, 2011, **115**, 6986.
203 A. Hassan, A. de la Escosura-Muñiz and A. Merkoçi, *Biosens. Bioelectron.*, 2015, **67**, 511.
204 Y. Liu, J. H. Dustin Lee, Q. Xia, Y. Ma, Y. Yu, L. Y. Lanry Yung, J. Xie, C. N. Ong, C. D. Vecitis and Z. Zhou, *J. Mater. Chem. A*, 2014, **2**, 16554.
205 C. H. A. Tsang, K. N. Hui, K. S. Hui and L. Ren, *J. Mater. Chem. A*, 2014, **2**, 17986.
206 C. Y. Zhai, M. S. Zhu, D. Bin, H. W. Wang, Y. K. Du, C. Y. Wang and P. Yang, *ACS Appl. Mater. Interfaces*, 2014, **6**, 17753.
207 C. G. Hu, X. Q. Zhai, Y. Zhao, K. Bian, J. Zhang, L. T. Qu, H. M. Zhang and H. X. Luo, *Nanoscale*, 2014, **6**, 2768.
208 S. S. Li, J. N. Zheng, X. H. Ma, Y. Y. Hu, A. J. Wang, J. R. Chen and J. J. Feng, *Nanoscale*, 2014, **6**, 5708.
209 A. Mondal and N. R. Jana, *ACS Catal.*, 2014, **4**, 593.
210 J. N. Tiwari, K. Nath, S. Kumar, R. N. Tiwari, K. C. Kemp, N. H. Le, D. H. Youn, J. S. Lee and K. S. Kim, *Nat. Commun.*, 2013, **4**, 2221.
211 S. Xu and P. Wu, *J. Mater. Chem. A*, 2014, **2**, 13682.